Available online at www.sciencedirect.com
ScienceDirect
Trans. Nonferrous Met. Soc. China 34(2024) 1−25
Transactions of Nonferrous Metals Society of China
www.tnmsc.cn

Effect of deformation processing on microstructure evolution and mechanical properties of Mg−Li alloys: A review

Zhan LIU, Jin-feng NIE, Yong-hao ZHAO

Nano and Heterogeneous Materials Center, School of Materials Science and Engineering, Nanjing University of Science and Technology, Nanjing 210094, China

Received 23 July 2022; accepted 13 March 2023

Abstract: As the lightest structural metal, Mg−Li alloys, possessing the advantages of high specific strength, high specific stiffness, good electromagnetic shielding, and damping properties, have a bright application prospect in automotive, aerospace, transportation, medical and other fields. However, the strength of Mg−Li alloys is lower when compared to other structural metals, which requires alloying or deformation treatment to enhance mechanical properties. The research progress of deformation processing of Mg−Li alloys is summarized, including the effect of conventional plastic deformation and severe plastic deformation on the microstructure and mechanical properties of Mg−Li alloys, the effect of strain and temperature in the deformation process on their microstructure and mechanical properties, and several grain refinement mechanisms of Mg−Li alloys. The problems encountered during the industrial application of Mg−Li alloys are discussed. Grain refinement and enhanced work hardening are still the primary means to improve the comprehensive performance. Several structural design strategies (heterogeneous structured materials) are highlightened, which will be helpful for the guidance of future innovations for Mg−Li alloys to reach high strength.

Key words: Mg−Li alloys; microstructure; mechanical properties; plastic deformation; grain refinement strengthening; severe plastic deformation

1 Introduction

With the continuous advancement of the global industrialization process, in addition to the requirements for metals in various industries, industrial manufactures also have certain requirements for the quality of metals. People are also searching for alternative metal materials that can meet the requirements of lightweight and environmental protection [1−3]. Magnesium−lithium (Mg−Li) alloys as the lightest metal in engineering applications, has a density of only 1.35−1.65 g/cm^3, which is two-thirds of the density of pure aluminum [4,5], two-ninths of the density of chromium-containing steel and two-fifths of the density of titanium alloys. In the 1960s, the US began to carry out large-scale research on Mg−Li alloys and developed Mg−Li alloys for armored-vehicle, airborne vehicles, and Lockheed Missiles and Space Company [6]. With the strong demand for lightweight structural parts and increasing attention to energy conservation and emission reduction, people now pay attention to Mg−Li alloys, an ultralight structural metal. Worldwide, many countries and regions have carried out different degrees of research on the properties and applications of Mg−Li alloys [7,8]. Chinese researchers have successfully prepared a variety of Mg−Li alloys [9]. A variety of Mg−Li alloys developed by Xi'an Sifang Ultra Light Material Co., Ltd. (China), LA141, LA43M, and LA103Z have

Corresponding author: Jin-feng NIE, Tel/Fax: +86-25-84303281, E-mail: niejinfeng@njust.edu.cn;
Yong-hao ZHAO, E-mail: yhzhao@njust.edu.cn
DOI: 10.1016/S1003-6326(23)66379-4

reached military standards in various properties and have been applied to aerospace, military industry, and other fields [10]. In transportation tools such as ships, vehicles, and airplanes, if metal structural workpieces made of magnesium alloy can be used, it is expected that the total weight of vehicles or ships will be greatly reduced, which can also save energy and achieve the purpose of environmental protection [11].

In the 1930s, German scientists mapped the phase diagram of Mg−Li alloy and determined the phase transformation of Mg−Li alloy [12]. The crystal structure of the Mg−Li alloy is changed from the original hexagonal closest-packed (HCP) structure to body-centered cubic (BCC) structure with more slip systems by adding an appropriate amount of LI [13]. When Li content is less than 5.7%, it is still HCP structure called α-Mg phase, and when Li content is more than 10.3%, it becomes BCC structure called β-Li phase. When Li content is between 5.7% and 10.3%, it has an HCP + BCC dual-phase (α-Mg + β-Li) structure [14]. The Mg−Li phase diagram is shown in Fig. 1 [15]. The HCP crystal structure of α-Mg phase is not easily deformed at room temperature. There are mainly slip systems of pure magnesium and most Mg alloys: $\{0001\}\langle 11\bar{2}0\rangle$ [16,17]. In addition, to slip, magnesium alloys with HCP crystal structure also rely on twins for plastic deformation. Twins mainly appear at $\{10\bar{1}2\}\langle 10\bar{1}1\rangle$ pyramidal crystal planes [18]. The addition of Li can reduce the axial ratio of Mg and the critical resolved shear stress (CRSS) of the non-basal slip, enabling the additional slip systems to become active and improving α-Mg ductility but decreasing its strength [19]. There are three primary slip systems of BCC crystal structure (for β-Li phase Mg−Li alloys): $\{110\}\langle 111\rangle$, $\{112\}\langle 111\rangle$, and $\{123\}\langle 111\rangle$. β-Li phase Mg−Li alloys can deform better than α-Mg phase Mg−Li alloys because they contains more slip systems. β-Li phase Mg−Li alloys have higher ductility but lower strength [20,21]. The dual-phase alloy has HCP and BCC structures and has good plastic deformation ability, high ductility, and low strength.

Due to the low strength of Mg−Li alloys and the absence of enough slip systems, the plastic deformation ability of Mg−Li alloys is poor, making them impossible to be used directly as structural workpieces in industrial applications. Therefore, scientists have modified the microstructure by adding a variety of alloying elements, thereby improving the performance of the Mg−Li alloys [22−25]. Many excellent cast Mg−Li alloys have been developed, such as Mg−6Al−2Sn−0.4Mn−Li alloys with high specific strength and stiffness [26], $Mg_{90}Li_6Si_4$ alloys with good hydrogen storage property [27], and Mg−9Li−3Al−1Zn magnesium alloys with excellent electromagnetic shielding properties [28]. In biomedicine, Mg−4Li−1Ca alloys with good bioabsorbable properties are expected to be popularized in the future due to their biocorrosion products not deleterious to the surrounding tissues and light weight [29]. Because of the formation of BCC structure, β-Li phase, and dual phase (α-Mg and β-Li) Mg−Li alloys can achieve better ductility and plastic processing performance [30]. However, they still failed to achieve the desired comprehensive properties, and a series of subsequent strengthening treatments are needed. To further enhance the formability and mechanical properties of Mg−Li alloys, various plastic processing methods were used, including rolling, extrusion, forging, rotary swaging, ECAP, and other plastic deformation methods, to improve the strength of Mg−Li alloys through grain refinement and work hardening [31−35].

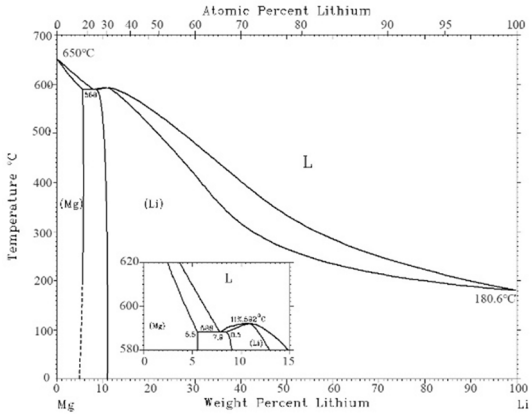

Fig. 1 Mg−Li phase diagram (Reproduced with permission from Ref. [15])

Although much literature has introduced the effects of alloying elements and heat treatment on the microstructure of Mg−Li alloys and how to improve the mechanical properties of Mg−Li alloys [9], there are few review articles on the effect of deforming processing on microstructure evolution and mechanical properties of magnesium

alloys. This work aims to introduce the properties and strengthening mechanisms of various Mg−Li alloys and provides some help for those who are interested in Mg−Li alloys.

2 Conventional plastic deformation

Generally, there are some defects in metals or alloys after melting, such as porosity and macro-segregation resulting in poor comprehensive performance and limited application [36]. To improve the property of the alloy, some subsequent heat treatment are usually carried out to eliminate these defects [37]. However, regulating the heat treatment temperature of Mg−Li alloys is challenging due to the lithium loss at high temperatures [38]. Plastic deformation can also eliminate casting defects like porosity, refine grains and introduce high density dislocation to enhance the properties of cast alloys [39]. Furthermore, strain-induced phase transformation in dual Mg−Li alloys has been shown [40]. The conventional deformation treatments include rolling, extrusion, rotary swaging, drawing, etc., and these methods can achieve high mechanical properties of Mg−Li alloys. The processing schematics are shown in Fig. 2.

2.1 Rolling

The rolling process is the most commonly used plastic forming process in the industry for the manufacturing of large-scale plates, sheets, and foils, and it is progressively being applied to the production of magnesium alloys [41]. The rolling process mainly uses the friction between the rolls and the material being processed to drag the material into the rolls, where it is exposed to considerable pressure from the two rolls and plastic deformation occurs [42,43]. The cross-section area is reduced, the shape is changed and the length is increased. The processing schematic is shown in Fig. 2(a). When magnesium alloys were subjected to vertical compressive stress during rolling deformation, the grains were elongated along the rolling direction [44]. The microstructure of the dual-phase Mg−Li alloy was also elongated in the rolling direction [45−47]. The microstructure was elongated significantly and a fibrous structure was formed when the applied rolling strain increased gradually, as seen in Fig. 3.

LIU et al [46] studied the effect of rolling strain on the microstructure and tensile properties of dual-phase Mg−8Li−3Al−2Zn−0.5Y alloy. The α-Mg phase was elongated in two directions, and the elongation along the RD direction was more obvious than that in the TD direction. Meanwhile, new AlLi and Al_2Y particles were precipitated and distributed homogeneously in the magnesium matrix. Because many dislocations are formed in the rolling process, the tensile properties are improved due to dislocation strengthening, and the movement of dislocations is impeded by precipitates, which further improves the material properties. With the continuous increase of rolling strain, the yield strength (YS) and ultimate tensile strength (UTS) continued to increase, but elongation (EL) significantly decreased. In this work, the tensile properties of magnesium alloy along the RD direction and TD direction are studied simultaneously, as seen in Fig. 4. Due to the significant anisotropy of HCP structure, the properties along RD direction are higher than those along the TD direction.

Rolling temperature also has a significant effect on the microstructure and property of Mg−Li alloys. Twins begin to disappear and are replaced by dynamically recrystallized grains as the deformation temperature rises. As the temperature increases, the dynamic recrystallization (DRX) mechanism of α-Mg phases changes from CDRX (continuous DRX) to DDRX (discontinuous DRX),

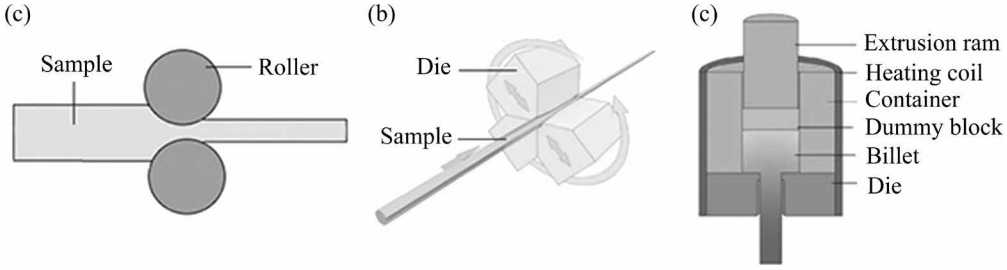

Fig. 2 Three conventional plastic deformation processes: (a) Rolling; (b) Rotary swaging; (c) Extrusion

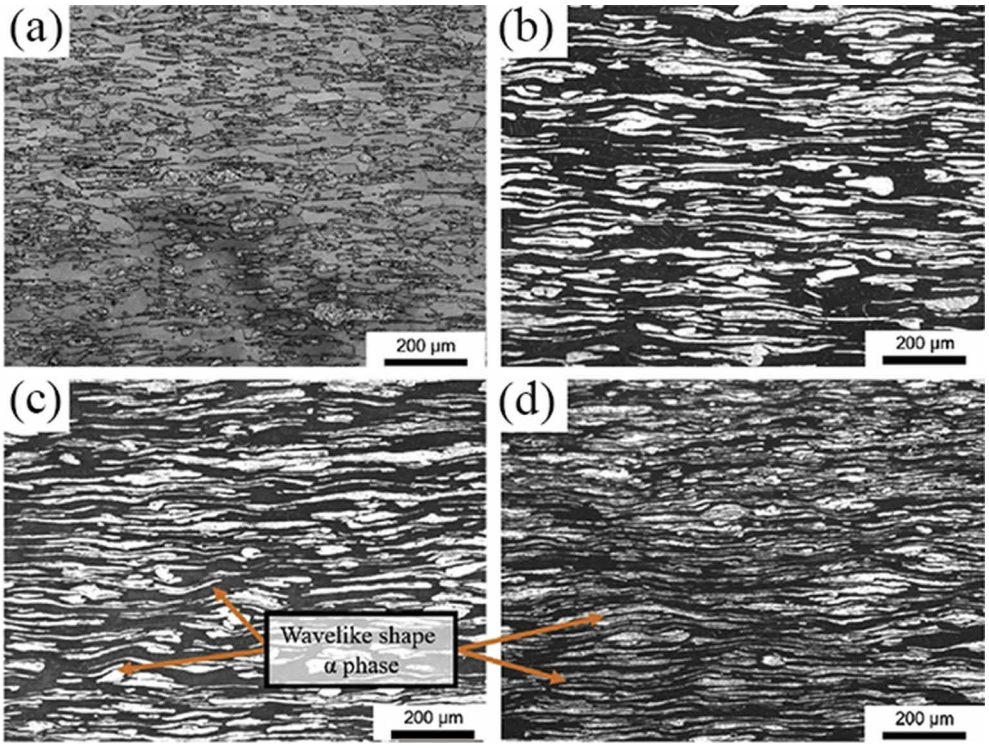

Fig. 3 Microstructures of dual-phase Mg−Li alloys with different rolling reductions: (a) 10%; (b) 30%; (c) 50%; (d) 70% (Reproduced with permission from Ref. [45])

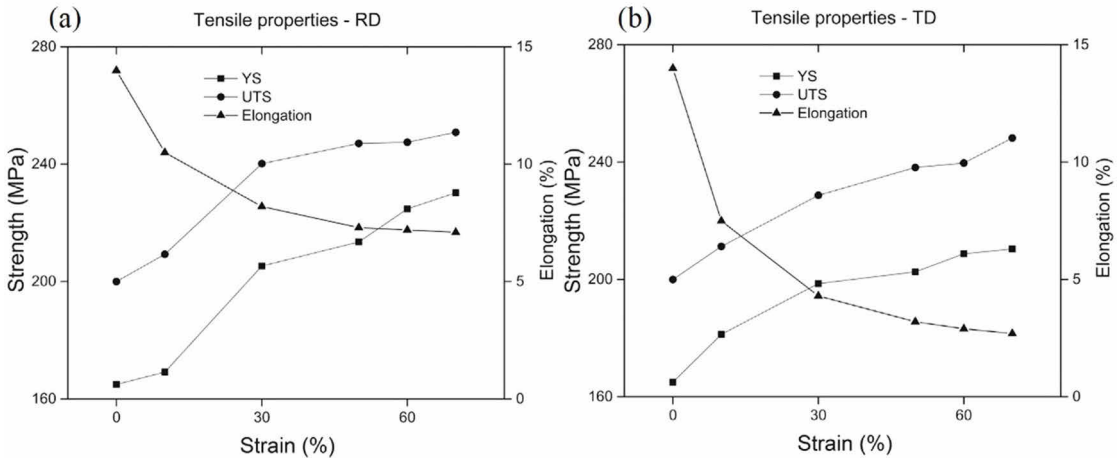

Fig. 4 Tensile properties of as-cast and as-rolled Mg−8Li−3Al−2Zn−0.5Y alloy with different rolling strains along RD and the TD (Reproduced with permission from Ref. [46])

according to ZHONG et al [48]. As temperature increases, the dynamic recrystallization mechanism of β-Li phases does not change. Meanwhile, UTS and EL of the alloy increase first and then decrease with the increase in temperature. The fine-grained strengthening and the dislocation strengthening related to DRX and imposed deformation are responsible for the improved mechanical properties. LI et al [49] investigated the texture and mechanical properties of rolled dual-phase LZ91 Mg alloys at various temperatures. Mg−Li alloys rolled at liquid nitrogen temperature have the highest YS and UTS, owing to the higher dislocation density obtained at liquid nitrogen temperature, as seen in Fig. 5(a). While at 200 and 300 °C, YS and UTS of the Mg−Li alloys decreased and the EL increased as the β-Li phase was recrystallized at higher rolling temperatures. Strain hardening of LZ91 alloys rolled at liquid nitrogen temperature is also higher than that of other alloys.

Different rolling processes also affect the properties of Mg−Li alloys. CAO et al [44] carried out hot-rolling on dual-phase Mg−Li alloy and then cold-rolling was further applied to it. The total reduction reached 60% and magnesium alloy with high strength and high elongation was finally obtained. JIANG et al [50] investigated the effects of varying rolling speed ratios on the structure and properties of the Mg−Li alloy. It is shown that with increasing speed ratio, the α-phase was first elongated into a fibrous structure and finally broken into bamboo-shaped grains due to the larger speed ratio, while the β-Li phase did not change significantly with increasing speed ratio. The mechanical properties of the Mg−Li alloys obtained with different rolling parameters (rolling strain, temperature, and rolling speed ratio) are given in Table 1. It is shown that liquid nitrogen temperature, high strain rate, and high strain may all improve the mechanical properties of the Mg−Li alloy. These factors can influence the DRX mechanism, hence refining the grains of Mg−Li alloy.

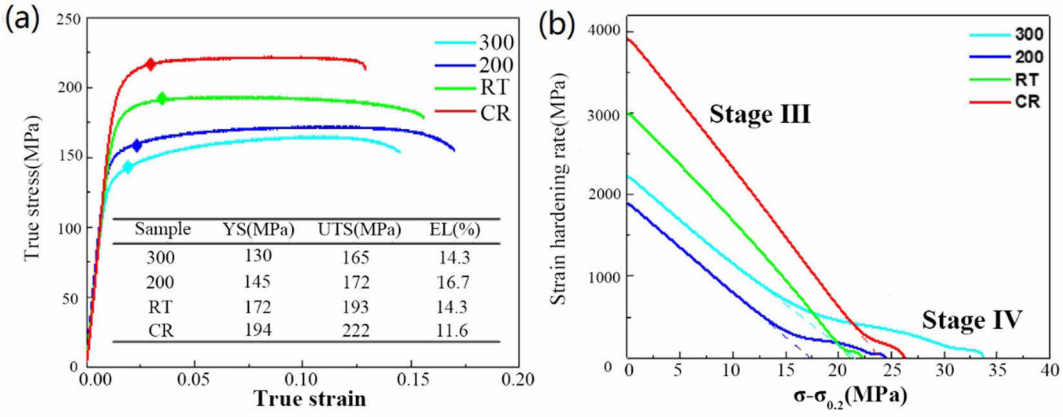

Fig. 5 True strain−stress curves (a) and strain hardening rate (b) of rolled samples at different temperatures (Reproduced with permission from Ref. [49])

Table 1 Tensile properties of as-rolled Mg−Li alloys with different deformation processings

Material	Phase	UTS/MPa	YS/MPa	EL/%	Rolling strain/%	Rolling temperature/K	Rolling speed ratio	Reference
LZ91	Dual-phase	222	194	11	70	77	1:1	[49]
		193	172	14	70	273	1:1	
		172	145	16	70	473	1:1	
		165	130	14	70	573	1:1	
Mg−8Li−3Al−2Zn−0.5Y	Dual-phase	209	169	11	10	473	1:1	[46]
		240	205	8	30	473	1:1	
		247	214	7	50	473	1:1	
		248	225	7	60	473	1:1	
		251	230	7	70	473	1:1	
Mg−14Li−1Al	β-Li	208		19	90	273	1:1	[51]
		223		26	90	77	1:1	
Mg−8Li−3Al−0.4Ca	Dual-phase	267	238	10	30	273	1:1.1	[50]
		260	235	13	30	273	1:1.2	
		263	226	14	30	273	1:1.3	
		264	227	15	30	273	1:1.4	
		265	230	15	30	273	1:1.5	

2.2 Rotary swaging

Rotary swaging is an industrial forming method commonly used to manufacture bars, pipes, and so on. The processing schematic is shown in Fig. 2(b). It is a process where the formed workpiece is obtained without or with only a minimum amount of processing and cutting. As the feedstock passes through the die, it is subjected to a continuous pulse of pressure along the radial direction of the mold. The cross-sectional area of the sample is reduced, and rotary swaging is a continuous and lossless metal forming method. It can produce a strain rate of up to 100 s^{-1} during production and produce high hydrostatic stress on the sample when the die is affected [52]. It not only makes the material obtain a work hardening effect, but also refines the grain size of material from coarse grain to ultra-fine grain, and thus improves the mechanical properties by fine grain strengthening [53]. Parts processed by rotary swaging can be applied in different fields, such as automotive industry where it is used for the manufacture of components, like axes, steering spindles, and gear shafts. Due to the HCP structure of magnesium and its alloys, the texture of the materials is also changed during the deformation process, and thus the mechanical properties of the materials are also enhanced [54,55]. GAN et al [56] conducted rotary swaging on as-cast pure magnesium, and its average grain size was eventually refined from 2.5 mm to 25 μm. Due to significant grain refinement and increased dislocation density, UTS was increased by three times and a strong {0001} basal fiber texture was observed. YANG et al [34] conducted rotary swaging on Mg−Li alloy and obtained an high strength Mg−Li alloy with UTS of about 405 MPa, far exceeding the known data of Mg−Li alloys processed by other methods. During the rotary swaging process, the material produces a large number of twins. These twins and stacking faults act as the main strengthening contributors, effectively blocking dislocation movement and thus providing ultra-high strength, as shown in Fig. 6.

However, during the rotary swaging process, the difference in microstructure and hardness in the central and edge regions requires further study. Rotary swaging enhanced the micro-hardness over HV 100 and usually formed a V-shaped distribution along the radial direction. CHEN et al [57] treated Mg−Li alloy by rotary swaging and measured the tensile properties of the central and edge regions. After five passes of die swaging, the central area of the alloy rod can be significantly strengthened, and the YS, UTS, and EL are 463 MPa, 511 MPa, and 7.6%, respectively. However, the YS, UTS, and EL at the edge region are 380 MPa, 441 MPa, and 7.9%, respectively. The enhancement effect was more obvious in the central region than in the edge. These results originate from the difference in loading mode and stress state at the center and edge regions. The grains in the marginal are subjected to a single direction (toward the center) load. However, due to the high frequency variation in the loading directions (almost all radial directions) during swaging, the grains in the central region are subjected to loading along all radial directions. The mechanical properties of the Mg−Li alloys obtained with different rotary swage parameters are given in Table 2. High strain effectively refines the grain and thus improves the mechanical properties of Mg−Li alloy, as shown in Table 2.

2.3 Hot extrusion

Mg−Li alloys can also benefit from hot extrusion to improve mechanical properties. It is possible to change the original structure and obtain fine grains by applying pressure at a required temperature. Other atoms, such as Si, Sm, and Gd, can also be doped to obtain a more homogenous phase distribution [58−60]. The refinement and dispersion strengthening were used to improve the properties of Mg−Li alloys [61−63]. Hot extrusion is the application of pressure to one end of the material placed in the extrusion cylinder, causing it to deform plastically. This can be used combined with powder metallurgy to produce the necessary material in addition to ingot processing [64]. The schematic diagram is shown in Fig. 2(c).

The extrusion parameters such as extrusion temperature and extrusion ratio have a significant influence on the structure and properties of Mg−Li alloys [65,66]. TANG et al [67] investigated the effect of extrusion temperatures from 473 to 623 K on the microstructure and mechanical properties of Mg−Li alloys, as shown in Fig. 7. With increasing extrusion temperature, the grains size of the two single-phase Mg−Li alloys increased. The grains size of Mg−5Li−5Al−2Zn−0.5Y alloys (α-Mg phase) was 16.1 μm and that of Mg−11.4Li−5Al−2Zn−

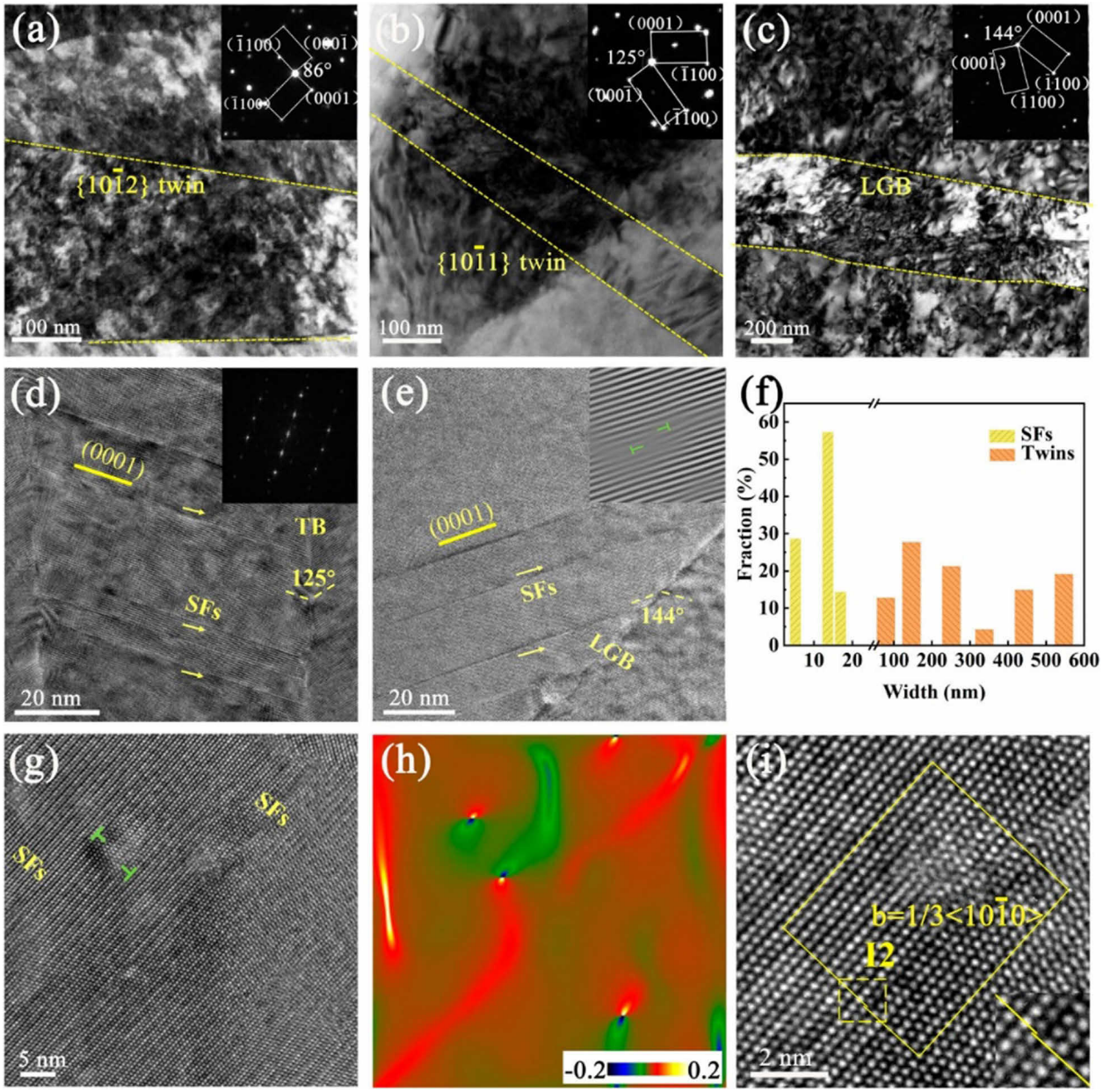

Fig. 6 Illustration of twinning and SFs strengthening mechanisms revealed by (HR) TEM: (a−c) Low magnified TEM images and corresponding SAED patterns of lamellar structures in RS-processed Mg−Li alloy; (d) HRTEM image and corresponding FFT showing SFs in {10$\bar{1}$1} twin; (e) HRTEM image and corresponding inverse fast-Fourier transform (IFFT) image of SFs in lamellar grain; (f) Variation of width for twins and SFs; (g, h) Atomic-scale TEM images of SFs and corresponding GPA analysis; (i) HRTEM image showing I2 fault bounded by 1/3⟨10$\bar{1}$0⟩ Shockley partials (Reproduced with permission from Ref. [34])

Table 2 Tensile properties of as-swaged Mg−Li alloys treated with different deformation processings

Material	Phase	UTS/MPa	YS/MPa	EL/%	Equivalent strain	Region	Reference
Mg−4Li−3Al−3Zn	α-Mg	441	380	7.9	0.24	Edge	[57]
		511	463	7.6	0.24	Center	
Mg−4Li−3Al−3Zn	α-Mg	368		7	0.32	Center	[34]
		405		5	0.32	Edge	
		375		6	0.25	Edge	

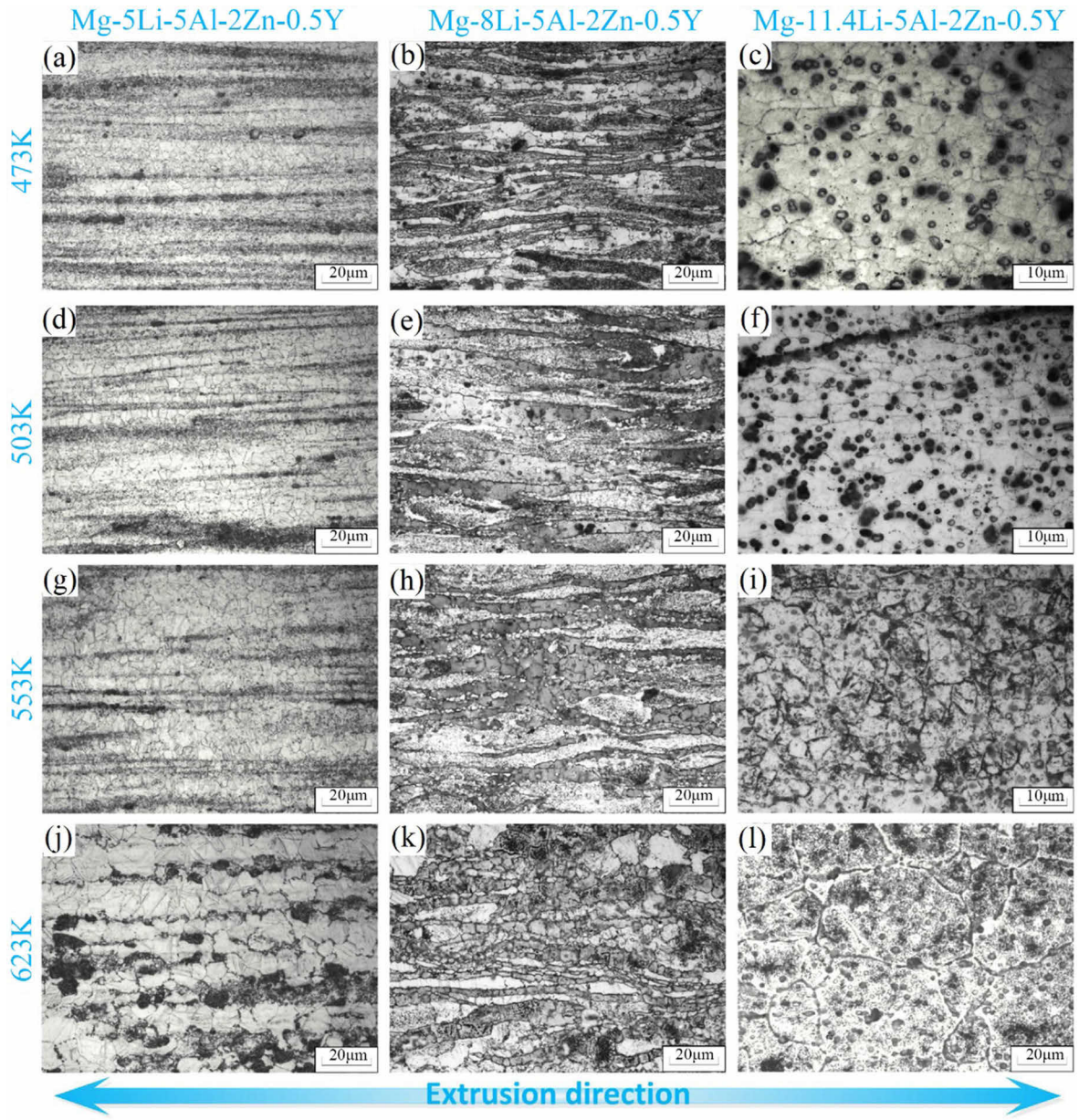

Fig. 7 Microstructures of three alloys extruded under different temperatures (Reproduced with permission from Ref. [67])

0.5Y alloys (β-Li phase) was 65.4 μm at the extruding temperature of 623 K. The dynamic recrystallization phenomenon became more obvious with increasing extruding temperature in both α-Mg phase and β-Li phase Mg−Li alloys. The dynamic recrystallization phenomenon also occurs in Mg−8Li−5Al−2Zn−0.5Y alloys (dual phase). The grain growth in α-Mg phase limited the development of β-Li phase at extruding temperature of 623 K, and thus the recrystallized grain size of β-Li phase did not show a noticeable increase. In the α-Mg phase Mg−Li alloy, the grains were elongated along the extrusion direction. In dual phase Mg−Li alloys, both α-Mg phase and β-Li phase elongated along the extrusion direction. UTS and YS decrease as the extrusion temperature increases, whereas EL increases for alloys with dual phases. For α-phase Mg−Li alloy, UTS and YS remain relatively steady while EL increases. The machinal properties of three alloys extruded at different temperatures are shown in Fig. 8. YANG et al [68] published a study showing similar results.

The influence of another key extrusion process parameter, the extrusion ratio, on the properties and microstructure of Mg−Li alloy was studied by FENG et al [69]. It is shown that α-Mg phase is

gradually elongated along the extrusion direction as the extrusion ratio increases. With increasing extrusion ratio, the UTS, YS, and EL of the dual-phase Mg−Li alloy increase and subsequently decrease, reaching a maximum at an extrusion ratio of 16:1.

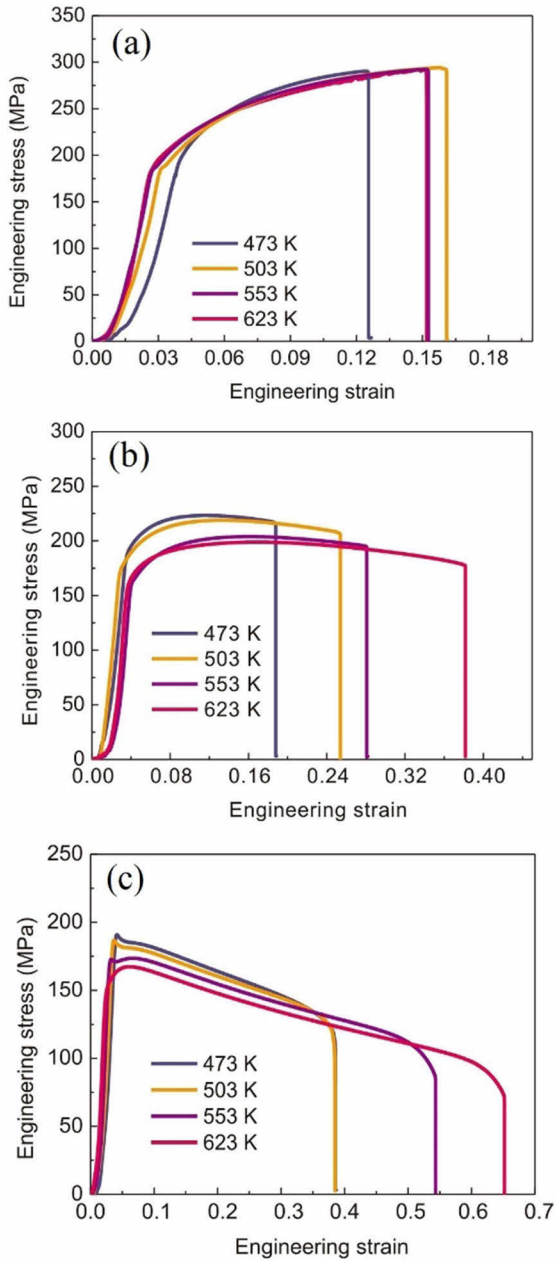

Fig. 8 Mechanical properties of three alloys extruded at different temperatures: (a) Mg−5Li−5Al−2Zn−0.5Y; (b) Mg−8Li−5Al−2Zn−0.5Y; (c) Mg−11.4Li−5Al−2Zn−0.5Y (Reproduced with permission from Ref. [67])

LI et al [70] investigated the effect of extrusion speed on the microstructure and mechanical properties of duplex Mg−Li alloys. After extrusion, the α-Mg phase grains are elongated parallel to the ED direction, and the β-Li phase grains undergo dynamic recrystallization. Because of the increase in extrusion speed, the temperature and the strain rate of the extrusion process increase, and the degree of plastic deformation and the degree of DRX in the edge zone gradually become larger, resulting in an increase in the average grain size on the edge. The average grain size of the LZ91 alloys extruded at different speeds is shown in Fig. 9. However, the grain size in the center first decreased and then increased. However, the UTS and EL decreased and then increased with the increase in extrusion speed. The mechanical properties of the Mg−Li alloys obtained with different extruding parameters are given in Table 3. The extrusion ratio, temperature, and speed can affect the DRX degree of the Mg−Li alloy. Mechanical properties can be further improved by extruding at low temperatures, high ratios, and high speeds.

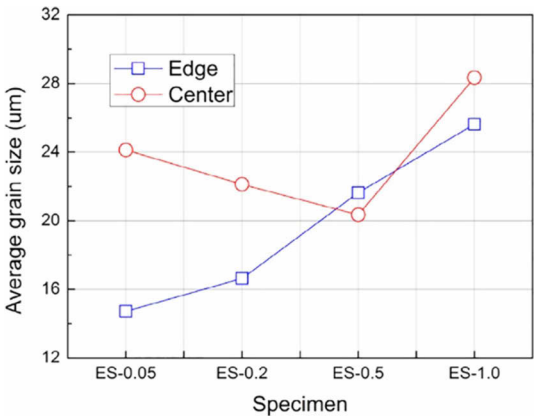

Fig. 9 Variation of average grain size of LZ91 alloys extruded at different speeds (Reproduced with permission from Ref. [70])

Generally, the grain size decreased with the increase of deformation degree (including rolling strain, extrusion strain, and swaging strain). In dual-phase Mg−Li alloys, the grains of both phases are also be elongated along the rolling and extrusion direction. The phase generally presents a thin strip along the deformation direction if the deformation direction does not shift. This tendency becomes more obvious as the degree of deformation increases. It is not always good to increase the deformation temperature since a decrease in plasticity is commonly accompanied by an increase in strength according to the Hall−Petch relationship. The mechanical properties of Mg−Li alloys needed to be improved with novel methods.

Table 3 Tensile properties of as−extruded Mg−Li alloys with different deformation processings

Material	UTS/ MPa	YS/ MPa	EL/ %	Extrusion ratio	Extrusion temperature/K	Extrusion speed	Reference
Mg−5Li−5Al−2Zn−0.5Y	291	204	13	17:1	473		[67]
	293	186	16	17:1	503		
	292	186	15	17:1	553		
	292	189	15	17:1	623		
Mg−8Li−5Al−2Zn−0.5Y	224	193	19	17:1	473		[67]
	217	183	25	17:1	503		
	205	167	28	17:1	553		
	199	165	38	17:1	623		
Mg−11.4Li−5Al−2Zn−0.5Y	191	189	38	17:1	473		[67]
	186	185	38	17:1	503		
	173	172	54	17:1	573		
	167	158	65	17:1	623		
Mg−9Li−3Al−2.5Sr	238		18	28:1	523		[68]
	223		20	28:1	573		
	208		22	28:1	623		
Mg−5Li−2Zn	216	142	18	79:1	573		[71]
	195	121	17	25:1	573		
	197	116	20	10:1	573		
Mg−9Li−1Zn	137		41	21:1	573	0.05 mm/s	[70]
	139		41	21:1	573	0.2 mm/s	
	142		44	21:1	573	0.5 mm/s	
	138		44	21:1	573	1 mm/s	
Mg−11Li−3Al−2Zn−1.5Nd−0.2Zr	145	150	42	23:1	503		[72]
Mg−9Li−3Zn−1Gd	187	149	44	25:1	473		[73]
Mg−9Li−6Zn−2Gd	201	165	36	25:1	473		
Mg−9Li−9Zn−3Gd	231	188	28	25:1	473		
Mg−8Li−3Al−2Zn−0.5Nd	243	208	24	25:1	473	2 m/min	[74]
Mg−8Li−3Al−0.5Mn	222	194	16	25:1	573	10 mm/s	[75]
Mg−8Li−3Al−0.5Mn−0.25Sr	220	186	19				
Mg−8Li−3Al−0.5Mn−0.5Sr	242	207	22				
Mg−8Li−3Al−0.5Mn−0.75Sr	265	175	17				
Mg−8Li−3Al−0.5Mn−1Sr	233	204	14				

3 Severe plastic deformation (SPD)

Severe plastic deformation (SPD) technology has advanced quickly over the last two decades, refining the coarse grains to ultrafine grains by applying large strain to cause severe plastic deformation of the material [76,77]. Equal channel angular pressing (ECAP), accumulative roll-bonding (ARB), tube cyclic extrusion compression (TCEC), friction stir processing (FSP), and high pressure torsion (HPT) are all commonly used severe plastic deformation processes [78]. SPD technique has been demonstrated in several

experiments to produce ultra-fine grain and ultra-high strength Mg−Li alloys [79].

3.1 Equal channel angular pressing (ECAP)

The schematic diagram of ECAP deformation is shown in Fig. 10(a). The sample is bent and extruded through a 90° corner under pressure, and after severe plastic deformation, high-density dislocations are generated and the grains are refined [80]. KARAMI and MAHMUDI [81] studied the microstructural and textural evolution of three Mg−Li alloys after ECAP. The grains of dual-phase Mg−Li alloys (LZ61 and LZ81) are refined significantly after ECAP, and the phase is homogenous due to continuous dynamic recovery and recrystallization. With an increase in the number of ECAP, the average grain size of β-phase Mg−Li alloy (LZ121) is reduced from 30.3 to 6.1 μm. Grain refinement improves the mechanical properties of the three alloys as the number of ECAP increases. A strong texture is formed in LZ121 after extrusion where (110) planes are mostly located perpendicular to the extrusion axis, as shown in Fig. 11(a). The texture of LZ121 becomes a randomly three-point intensity texture after ECAP, as shown in Figs. 11(b, c).

Currently, ECAP improves the properties of Mg−Li alloys by focusing on grain refinement. The purpose of ECAP is to improve the poor mechanical properties of Mg−Li alloys. Combined processing can be used to change the structure and hence enhance the properties to broaden the range of applications for Mg−Li alloys. FURUI et al [82] combined the extrusion and ECAP processes to obtain Mg−Li alloy with extremely high elongation (~1780%), as shown in Fig. 12. The mechanical properties of the Mg−Li alloys obtained with different ECAP parameters are given in Table 4.

3.2 High-pressure torsion (HPT)

High-pressure torsion (HPT) deformation is the most typical and representative deformation method with the strongest grain refinement ability among available SPD processes [79]. The processing diagram is shown in Fig. 10(b). The material is placed in the die chamber at room

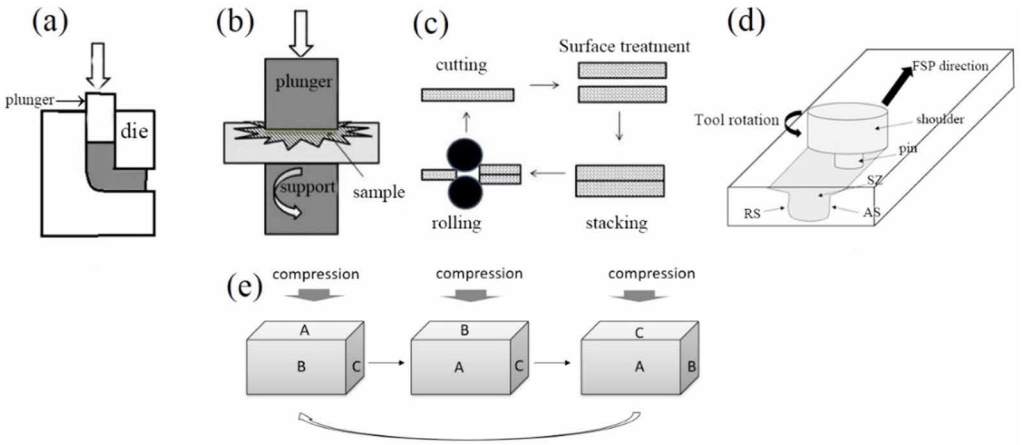

Fig. 10 Several SPD processes: (a) ECAP; (b) HPT; (c) ARB; (d) FSP; (e) MDF

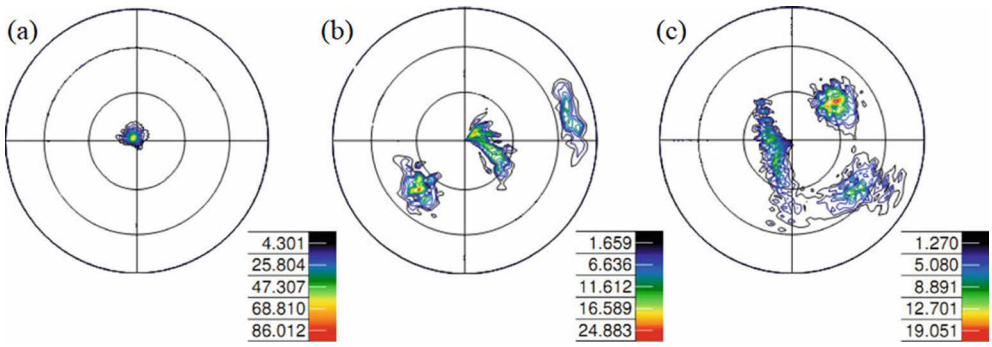

Fig. 11 (110) pole figures of LZ121 alloy after extrusion (a), 2 ECAP passes (b), and 4 ECAP passes (c) (Reproduced with permission from Ref. [81])

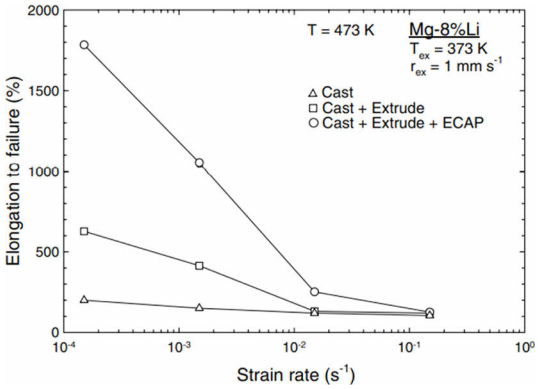

Fig. 12 Variation of elongation to failure with initial strain rate at testing temperature of 473 K for samples in Cast, Cast + Extrude and Cast + Extrude + ECAP conditions (The extrusion was conducted at 373 K using an extrusion speed of 1 mm/s) (Reproduced with permission from Ref. [82])

Table 4 Tensile properties of as-ECAPed Mg−4Li−4Al−2RE alloys with different deformation processings [83]

Phase	UTS/MPa	YS/MPa	EL/%	ECAP pass	Temperature/K
Dual-phase	199	175	0.9	1	503
	205	182	0.9	2	483
	218	193	0.8	4	458
	219	191	0.9	8	458
	221	192	1	12	458

temperature or a specific temperature and the pressure is applied in the direction perpendicular to the plane of the sheet [84]. At the same time, the rotating lower die gives certain shear stress to generate a shear torque, so that the material is deformed under the dual action of pressure and shear force. Although HPT can refine grain and increase mechanical properties, little investigation has been done on the application of HPT to Mg−Li alloys. MATSUNOSHITA et al [85] studied the impact of HPT on the microstructure and mechanical properties of a dual-phase Mg−Li alloy, in which HPT refined the average grain size to 500 nm. Under various tensile test conditions, the mechanical properties were investigated, with superplasticity reaching 1330% at 473 K, as shown in Fig. 13. The HPT treated samples have a microhardness ranging from HV 57 to HV 63.

SRINIVASARAO et al [86] conducted HPT deformation on a variety of Mg−Li alloys (including

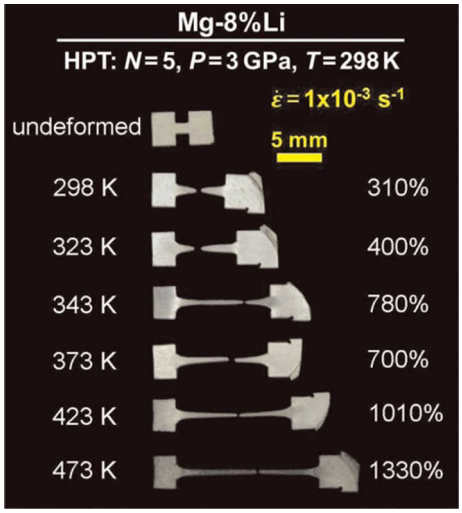

Fig. 13 Appearance of HPT-processed samples after pulling to failure at different temperatures with initial strain rate of 1×10^{-3} s^{-1}, including appearance of undeformed sample (Reproduced with permission from Ref. [85])

dual-phase and β-phase Mg−Li alloy) at room temperature and found that the transformation from β phase to α phase occurred in the β-phase Mg−Li alloys under pure compression. This phase transformation is caused by pressure and becomes more obvious with increasing pressure, as shown in Figs. 14(a, b). In dual-phase Mg−Li alloy, no such phase transformation occurred.

3.3 Accumulative rolling bonding (ARB)

The ARB technology is an easy industrial method for preparing fine-grained plates and sheets and is favored because of its low cost, easy operation, and low equipment requirements. This technology can be widely used to process various common metal materials, such as steel, aluminum alloy, titanium alloy, magnesium alloy, and dissimilar metal composites [87−89]. In addition to obtaining ultra-fine grains to enhance the properties, ARB technology can also improve the interface bonding ability through transition of intermetallic compounds formed between the interfaces. Thus, the mechanical properties of the materials are further improved [90,91]. During the ARB bonding process, there are many mechanisms, including the energy barrier mechanism, diffusion bonding mechanism, recrystallization bonding mechanism, and dislocation mechanism [91,92]. Its processing diagram is shown in Fig. 10(c). Firstly,

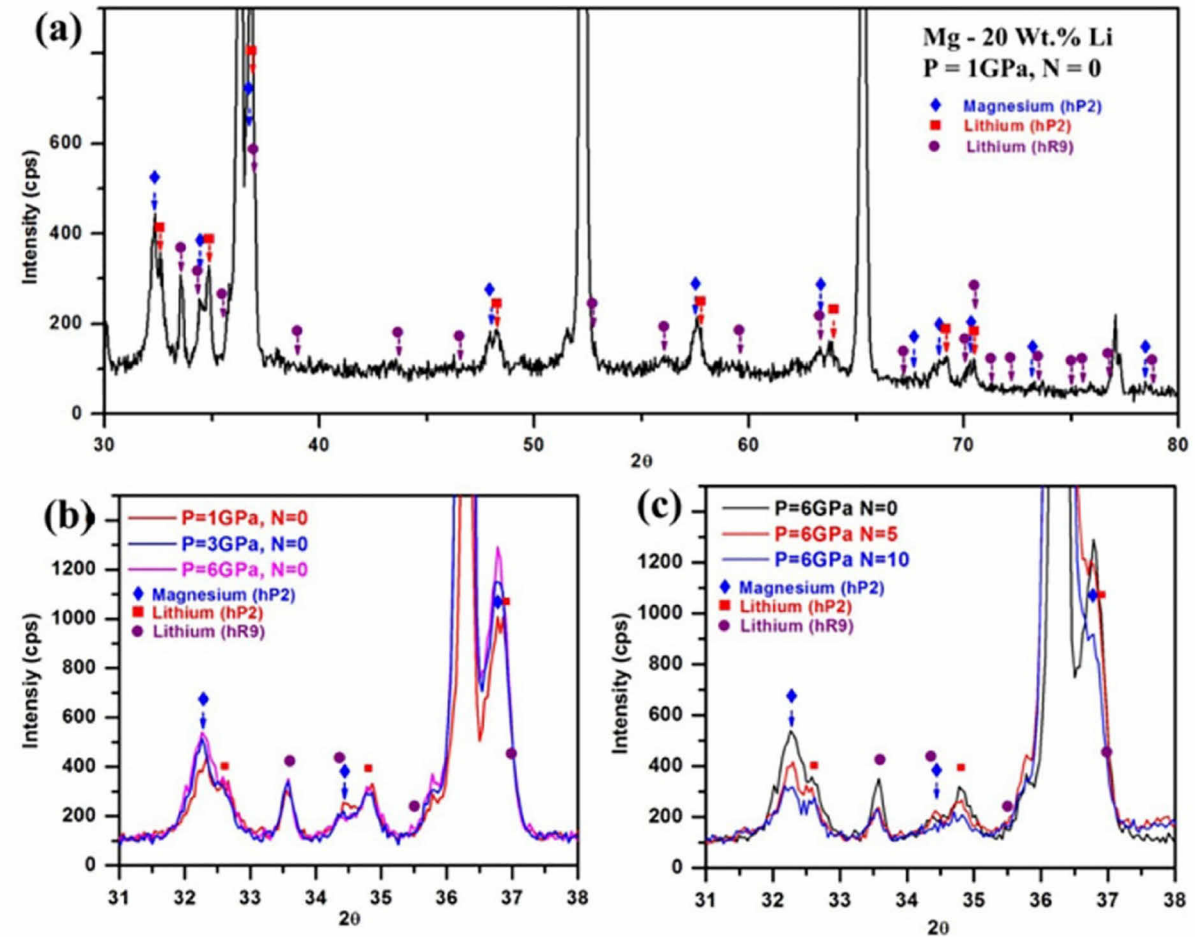

Fig. 14 XRD patterns corresponding to Mg−20wt.%Li alloy processed by HPT using different pressures and number of anvil turns: (a) P=1 GPa and N=0; (b) P=1, 3 and 6 GPa and N=0; (c) P=6 GPa and N=0, 5 and 10 (Reproduced with permission from Ref. [86])

the original sheet is cut into the same size, polished, degreased, and subjected to other surface treatments, those sheets are fixed with rivets or iron wire, and then the composite sheet was rolled at a certain temperature and pressure. This process is repeated. TSUJI et al [93] summarized the changes in geometric parameters such as the total number of layers, the total strain, and the equivalent strain with the cycle number in the process of ARB. When the original thickness of the sheet is 1 mm, after 10 cycles, the total number of sheet layers reaches 1024, and the total strain can reach 99.9%.

ZHONG et al [94] conducted ARB treatment on α phase and β phase Mg−Li alloy to obtain a multilayer sheet with good interfacial metallurgical bonding, and the microstructure of the ARBed α/β Mg−Li sheets is shown in Fig. 15. The hardness of the ARB6 Mg−Li alloy reached HV 64.7. The yield strength, tensile strength, and elongation of the ARB6 sheet are 138, 244 MPa, and 15.08%. The improvement in mechanical properties is ascribed to fine grain strengthening and strain hardening in the process of ARB. It is worth mentioning that a transverse shear band is formed near the interface due to the difference in plastic deformation flow between α single-phase Mg−Li alloy and β single-phase Mg−Li alloy. The dislocation density near the interface is obviously larger than that in the position far away interface, and the TEM images of the ARBed α/β Mg−Li sheets are shown in Fig. 16.

Another factor that affects the mechanical properties of ARBed alloys is the number of layers in the first rolling process. ZHENG et al [95] study the different numbers of layers in the first rolling process of Mg−14Li−3Al−2Gd and found that the four-layer accumulative roll bonding (FARB) is better than the two-layer accumulative roll bonding (TARB) about accumulative layers, the total number

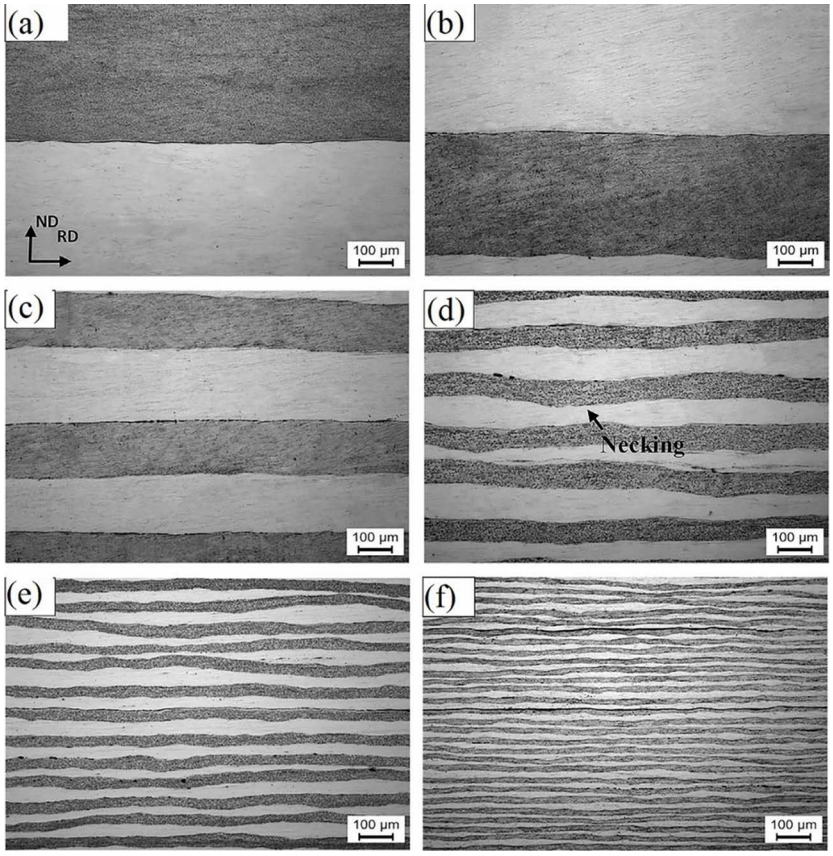

Fig. 15 Microstructures of ARB-processed α/β Mg−Li sheets: (a) ARB1; (b) ARB2; (c) ARB3; (d) ARB4; (e) ARB5; (f) ARB6 (Reproduced with permission from Ref. [94])

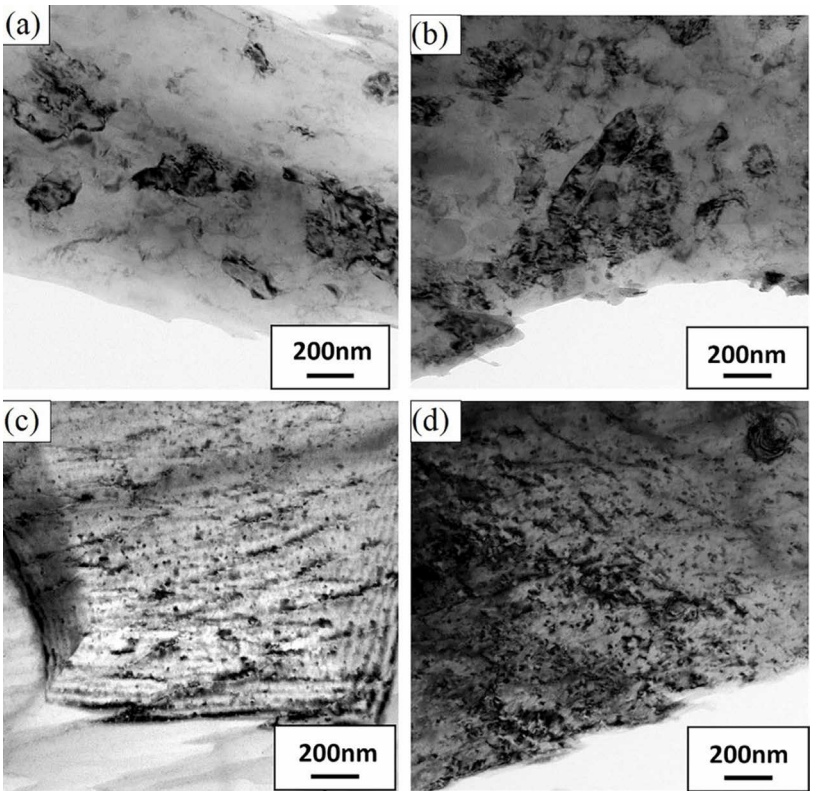

Fig. 16 TEM images of RD−ND plane of LA51/LA121 sheet: (a) LA51 alloy far away from interface; (b) LA51 alloy near interface; (c) LA121 alloy far away from interface; (d) LA121 alloy near interface (Reproduced with permission from Ref. [94])

of interfaces, interface spacing, total deformation, and equivalent strain. The grain size of FARBed alloy is refined than that of TARBed alloy caused by higher interface spacing. The UTS, YS, EL, and hardness of FARBed alloy are higher than those of TARBed alloy in the same cycle of ARB, as shown in Fig. 17. Mechanical properties are improved due to strain hardening and grain refinement strengthening.

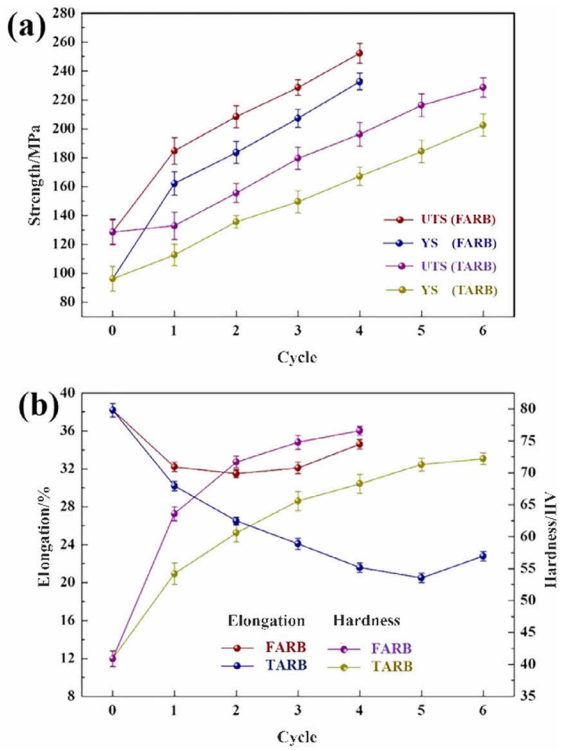

Fig. 17 Comparison of mechanical properties of TARB-processed and FARB-processed Mg−14Li−3Al−2Gd sheets: (a) YS and UTS; (b) EL and hardness (RD−TD plane) (Reproduced with permission from Ref. [95])

In addition to different kinds of Mg−Li alloys with ARB treatment, quite a few researchers also choose to combine Mg−Li with other alloys using ARB, such as Al [96], Al−Li [97], MWCNTs [98], and Ta [89]. Owing to their combination with Mg−Li, these alloys not only have improved mechanical properties, electromagnetic shielding effectiveness, and shielding of the high-energy electron, but also have decreased density [99]. This significantly helps to broaden the applications for Mg−Li alloys. The mechanical properties of the Mg−Li alloys obtained with different ARB parameters are given in Table 5. The accumulated strain during the rolling process can affect the interlayer thickness, interface state, size and morphology of internal grains and particles, and grain boundary composition of the material, which can then significantly improve the strength of the material through grain refinement strengthening, dislocation increment strengthening, second phase strengthening, and other strengthening mechanisms.

Table 5 Tensile properties of as-ARBed Mg−Li alloys with different deformation processings

Material	UTS/ MPa	EL/ %	Number of layers	Reference
Mg−Li−Al/Al−Li	308	17.4	16	[97]
Mg−5Li−1Al/ Mg−12Li−1Al	244	15.1	32	[94]
Mg−9Li−1Al	161	14.1	2	[100]
	173	9.7	4	
	192	6.3	8	
	219	4.3	16	
Mg−14Li−3Al−2Gd	181		4	[92]
	224	27.4	32	
Mg−9Li−1Zn	235	22.8	2	[101]
	290	15.7	32	
Mg−8Li−3Al−1Zn	287	13	32	[102]
Mg−5Li−1Al	306	16	64	[103]
Mg−5Li−1Al	318	8.4	64	[104]

3.4 Multi-directional forging (MDF)

Forging is a traditional approach to the treatment of cast defects in industrial production. Multi-directional forging (MDF) is a method to obtain severe plastic deformation based on forging. MDF is simple to operate and can produce large ultra-fine grains with high efficiency through multi-pass. The sample is subjected to pressure and deformation in three directions during MDF processing [105,106]. After each forging pass, the sample is tilted by 90°. The MDF process is shown in Fig. 10(e). MDF has been applied to several magnesium alloys such as AZ31 [106], Mg−13Gd−4Y−2Zn−0.5Zr [107], Mg−Li−Al−Zn−Sr [108], Mg−6.4Li−3.6Zn−0.37Al−0.36Y [109], and Mg−Li−Al [110], to modify their mechanical properties. CAO et al [111] found that the deformation mechanisms of MDF in the Mg−2.76Li−3Al−2.6Zn−0.39Y alloy are intense mechanically shearing fragmentation and incomplete dynamic recrystallization. The size of the coarse grain first

decreased and then increased with the increased MDF pass. At the 6th pass, the average grain size of coarse grain is a minimum of about 13.7 μm. The volume fraction of DRXed fine grain increased after MDF. The DRXed fine grains and unDRXed coarse grains formed a bimodal structure in Mg−Li alloy, as shown in Figs. 18(e−h). Mechanical properties of Mg−2.76Li−3Al−2.6ZN−0.39Y alloy are enhanced by MDF processing, as shown in Fig. 18(i). The UTS, YS, and EL of the 6th pass MDF are 256 MPa, 189 MPa, and 38.5%. Other researchers demonstrated that the bimodal microstructure can improve the strength and ductility by the hetero-deformation induced (HDI) stress strengthening effect [112,113].

MEHRABI et al [114] studied the superplastic behavior of LZ81 alloy by MDF. LZ81 alloy not only obtained refined grains but also increased fraction of high angle grain boundaries (HAGBs) from 54% to nearly 83% after MDF processing, as shown in Figs. 19(a−d). The LZ81 alloys after MDF showed a more significant work softening region compared with the extrude condition, as shown in Figs. 19(e, f). Grain boundary sliding accommodated by grain boundary diffusion is the dominant superplastic deformation mechanism.

3.5 Friction stir processing (FSP)

Friction stir processing (FSP) is a solid-state processing technology that uses the basic principle of friction stir welding (FSW) to modify the microstructure and properties of alloys, initially applied to aluminum alloy [115]. Figure 10(d) shows the schematic diagram of FSP, which uses specifically designed pin and shoulder as rotating tools [116]. Frictional heat softens the material, which flows from the front of the pin to the back of the pin as the tool rotates. Material flow around the pin may be pretty complex with different tool shapes [117]. The material is subjected to severe plastic deformation and high temperature during FSP, resulting in fine and equiaxed recrystallized grains. FSP is more flexible than ECAP, ARB, and HPT since the dimensions, contours, and original shape of the workpiece are not changed during the FSP process [118]. FSP has been successfully optimized to enhance the microstructure of many alloys [119−121].

The quality of the welded joints formed varies depending on the tool material. ZHOU et al [122] reported that WC cemented carbide tools outperformed steel tool joints in a comparative examination. A steel tool fails to form a valid joint

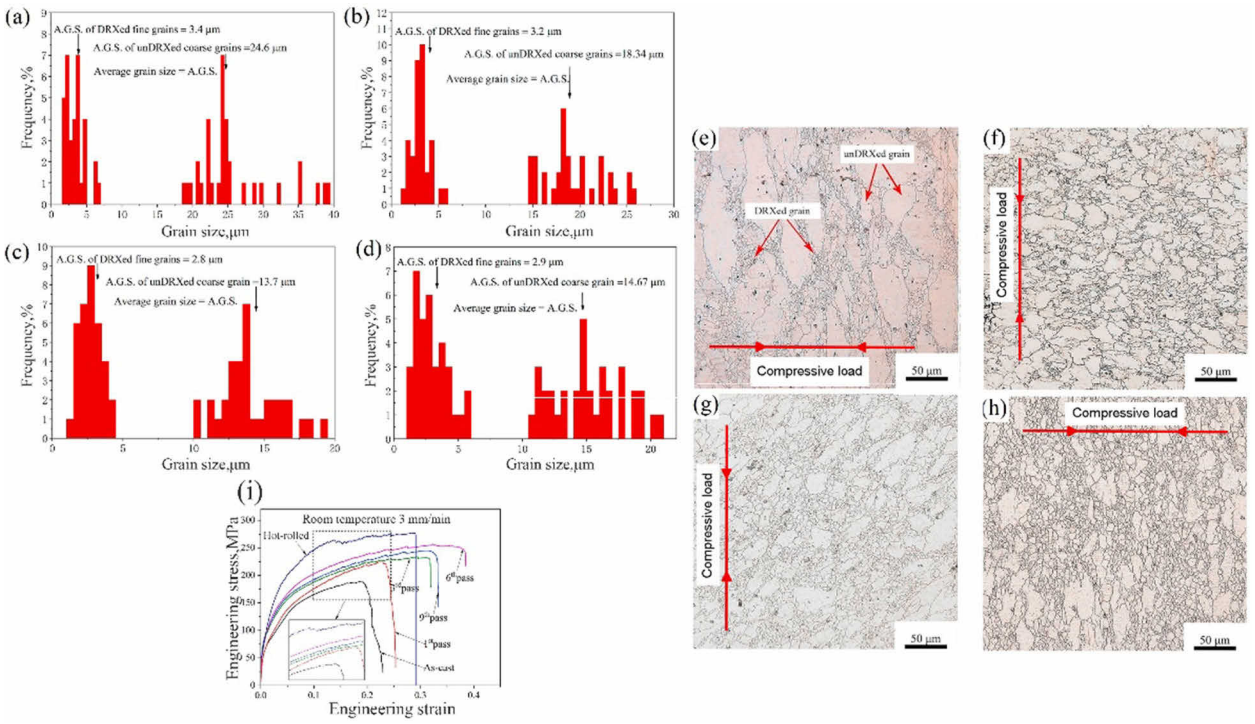

Fig. 18 Bimodal grain distribution and OM microstructures of LAZY330 alloy after MDF: (a, e) 1st pass; (b, f) 3rd pass; (c, g) 6th pass; (d, h) 9th pass; (i) Engineering stress−strain curves after MDF and hot rolling (Reproduced with permission from Ref. [111])

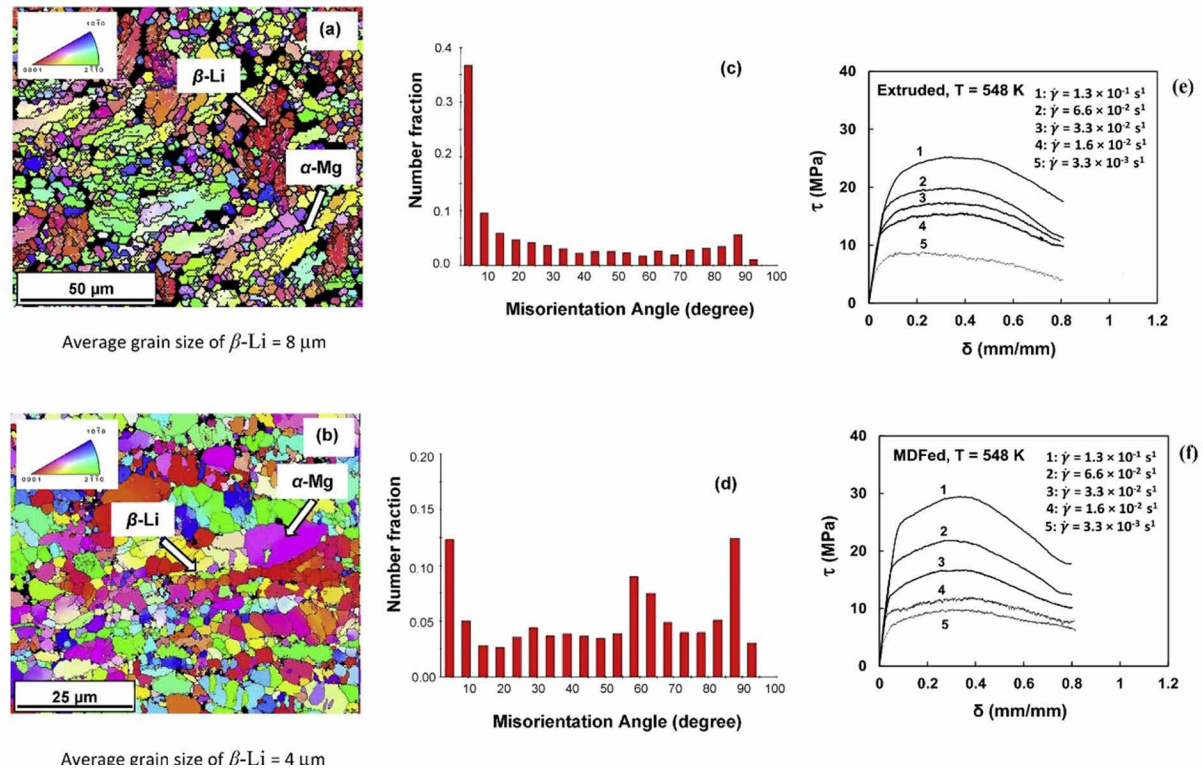

Fig. 19 EBSD orientation maps, corresponding grain boundary misorientation distribution and Typical SPT curves at 548 K and various shear strain rates of extruded (a, c, e), and MDF (b, d, f) processed alloys (Reproduced with permission from Ref. [114])

and produces many defects visible to human eye, whereas a WC cemented carbide tool provides a defect-free joint. The material adhering to the steel tool after FSW produces the defects. The wettability of the welding material and the tool surface does have a direct effect on the joint formation [123]. Therefore, a WC cemented carbide tool with a low wettability match is suitable for FSP treatment of Mg−Li alloys.

Several zones are formed in the material after FSP, including the stir zone (SZ), the thermal-mechanical affected zone (TMAZ), and the base metal (BM). Because the BM zone is away from the shoulder and pin, it takes less heat energy, maintaining the strip-shaped structure. The SZ undergoes friction, generating high temperatures, and dynamic recrystallization occurs in the grains, resulting in a microstructure that transforms from primitive coarse grains to fine equiaxed grains. The average grain size of the α-Mg phase within the SZ is refined from 5.7 to 2.1 μm, while the average grain size of the β-Li phase is refined from 11.9 to 2.2 μm, as shown in Fig. 20 [124].

Friction between the pin and the shoulder generates heat in FSP, softening the base metal. The rotation rate and travel speed are the two main factors that influence the heat input. LI et al [125] studied the microstructure and mechanical properties of dual-phase Mg−Li alloys under different welding parameters. Equiaxed grains are formed in the SZ of the Mg−Li alloy after FSP; however, the size of the equiaxed grains is affected by different parameters. As the rotation rate increases, the heat input increases as well, resulting in the large average size of equiaxed grains. At a rotation rate of 800 r/min, the average grain size of the β-Li phase reached 7.26 μm; whereas at 400 r/min, the average grain size of the β-Li phase reached 4.23 μm (when using the tool shoulder diameter of 16 mm, pin diameter in the root of 6.1 mm, and pin diameter in the tip of 5.5 mm). When the tool size and rotation rate are low, the effect of travel speed on the microstructure in the SZ of Mg−Li alloy is less significant than that of rotation rate. The volume fraction of the two phases of the Mg−Li alloy is also affected by the FSP; as the tool size and rotation rate increase, the volume fraction of the α-Mg phase decreases. Grain

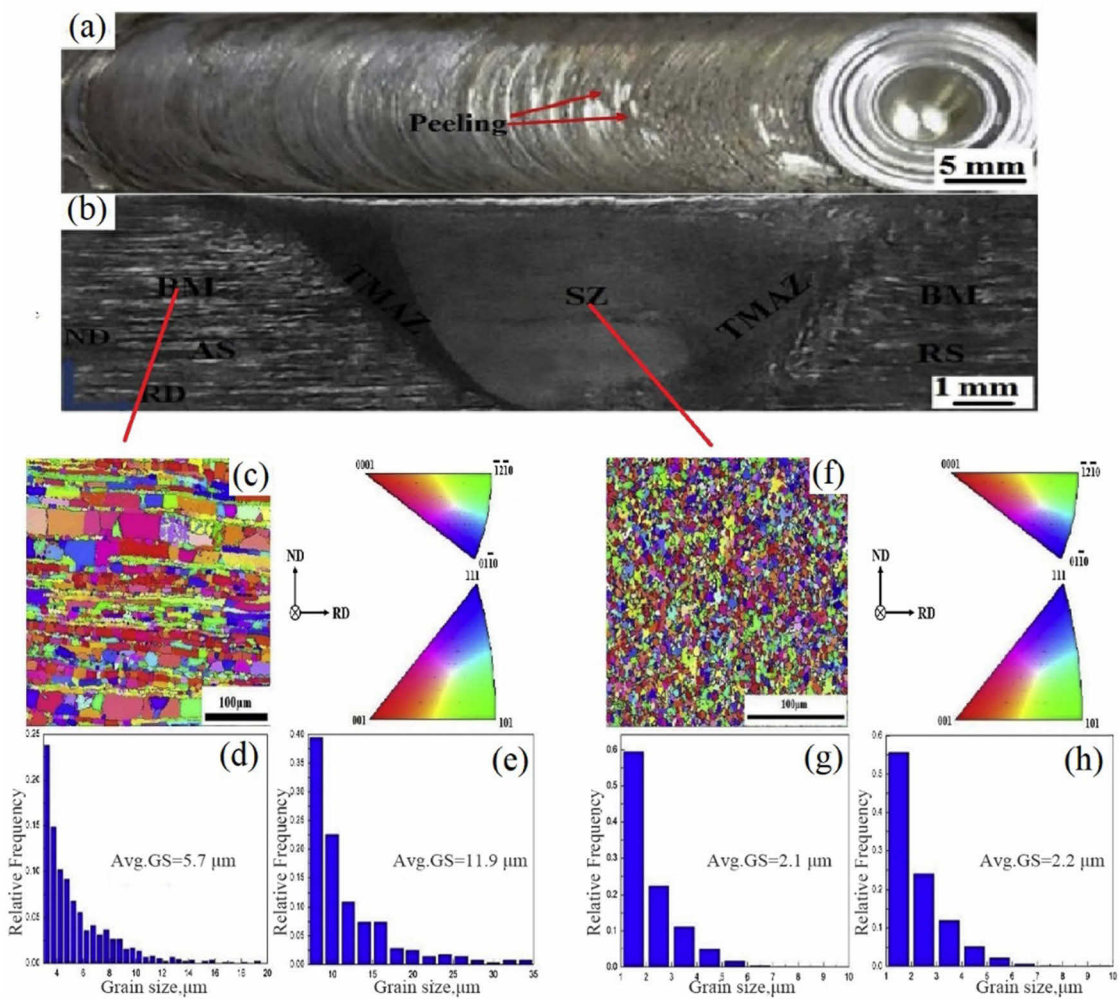

Fig. 20 Optical image of surface of processed region (a); Cross-sectional macrograph of friction stir processed specimen (b); Orientation map of BM (c) and SZ center (f); Grain size distribution of α-Mg phases in BM (d) and SZ center (g); Grain size distribution of β-Li phases in BM (e) and SZ center (h) (Reproduced with permission from Ref. [124])

refinement and solid solution strengthening improve mechanical properties of the Mg−Li alloy. YS and UTS increase as the rotation rate increases, while EL decreases, as shown in Fig. 21. ZHOU et al [122] studied the mechanical properties and fracture behavior of Mg−Li alloys. The digital image correlation (DIC) test shows that when the tensile strain increases, the local plastic strain is gradually concentrated in the BM caused by the difference in strength between the SZ and BM. The specimen eventually fractures at the interface between BM and SZ. The mechanical properties of the Mg−Li alloys obtained with different FSP parameters are given in Table 6. Multi-pass and high rotation rates have a considerable impact on grain size and mechanical properties of the Mg−Li alloys.

The severe plastic deformation technology can further refine the grain size of the material and increase the dislocation density, and then obtain higher tensile strength than conventional plastic deformation technology due to the Hall−Patch relationship and strain-hardening strengthening. Furthermore, SPD technology effectively avoids the issue of sacrificing plasticity to improve strength in conventional deformation technology by enhancing both the strength and toughness of the material at the same time to a certain limit. In some SPD processes (HPT and FSP), the β-Li phase is fractured in a large volume, and then α-Mg and β-Li phases show random distribution after deformation. However, in the ARB, ECAP, and

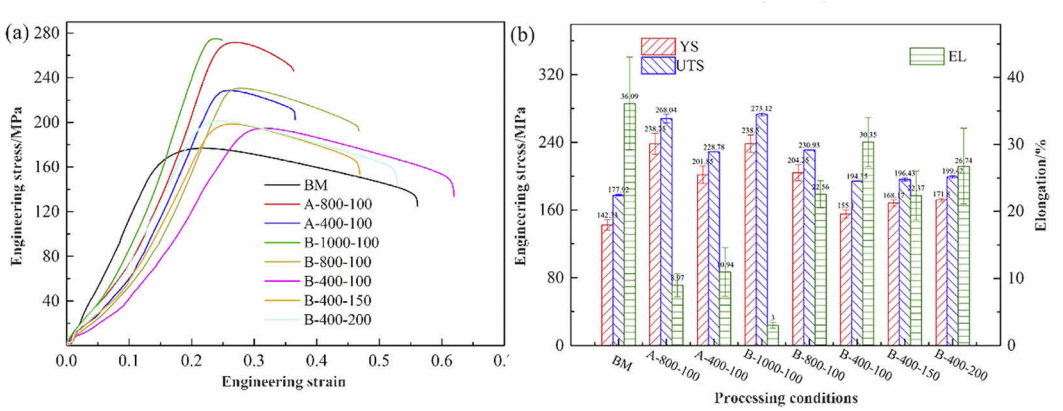

Fig. 21 Engineering stress−strain curves (a) and YS, UTS and EL (b) of BM and FSPed samples (Reproduced with permission from Ref. [125])

Table 6 Tensile properties of as-FSPed Mg−Li alloys with different deformation processings

Material	UTS/ MPa	EL/ %	Rotation rate/ (r·min^{-1})	Travel speed/ (mm·min^{-1})	Tool shoulder diameter/mm	Pin length/mm	Pin diameter in root or tip/mm	Reference
Mg−10Li−3Al−3Zn	268	9	800	100	16	3	6.1/5.5	[125]
	229	11	400	100	16	3	6.1/5.5	
	273	3	1000	100	12	3	3.9/3.5	
	231	23	800	100	12	3	3.9/3.5	
	194	30	400	100	12	3	3.9/3.5	
	196	22	400	150	12	3	3.9/3.5	
	199	27	400	200	12	3	3.9/3.5	
Mg−9Li−1Zn	150	31	100	100	15	6	2.8/2.8	[122]
	150	30	200	100	15	6	2.8/2.8	
	151	33	300	100	15	6	2.8/2.8	
Mg−9Li−1Zn	305	28	1800	60	15	6	5.7/5.7	[124]
Mg−9Li−1Zn	218	41	30	10	15	2.8	6/6	[126]

MDF processes, the β-Li phase still shows a preferred distribution along the deformation direction (without changing the deformation direction).

4 Conclusion and outlook

Various plastic deformation processings of Mg−Li alloys with special analyses of the impact on microstructure and mechanical properties were reviewed. It was noted that mechanical properties were improved by work hardening and grain refinement. The dynamic recrystallization (DRX) is the main grain refinement mechanism for Mg−Li alloys. Both accumulation of plastic deformation and deformation temperature can accelerate DRX in deformation processing. The severe plastic deformation technology can accumulate more plastic deformation and thus further refine the grains. DRX occurred readily at a relatively high deformation temperature in the deformation process. Another factor that should be taken into consideration in plastic deformation is the strain rate. High strain rates usually induce the formation of deformation twins, which can further improve the mechanical properties of the alloys. Mg−Li alloy has a small density and a broad application prospect in aerospace, military, automotive, medical equipment, and other fields. However, the existing magnesium alloy structural parts have certain defects in material strength, corrosion resistance,

room temperature workability, and other aspects, which restrict the further promotion and application of magnesium alloy structural parts. Understanding the influence of various deformation processes and deformation parameters on microstructure and mechanical properties will guide researchers in the development of new high-performance, low-cost Mg−Li alloys. It can accelerate the scaling up of new types of Mg−Li alloys from the laboratory to industrial production. This work seems to create some new insights into academics and industry to improve the mechanical properties of Mg−Li alloys.

(1) Most studies on the mechanical properties of Mg−Li alloys have been focused on LA, LAZ, and LZ alloys, recently. It is necessary to conduct more in-depth theoretical research on micro-structure parameters such as dislocations, twins, stacking fault energy, texture, and plastic deformation mechanism of Mg−Li alloys and establish the relationship model among components, processing technology, microstructure, and properties. Furthermore, the strain behavior and stress distribution during deformation can be analyzed by the finite element model.

(2) In the future, it is necessary to develop more advanced plastic processing methods (including nano-structure preparation, design of heterogeneous structure, and severe plastic deformation treatment) to improve the comprehensive performance base on alloying. If researchers fully use the high plasticity of Mg−Li alloys and combine them with advanced plastic deformation technology, the performance of Mg−Li alloys will be much superior. Due to the hetero-deformation induced (HDI) strengthening and HDI hardening of HS in microstructure and improvement of properties, it shows good potential to be vastly implemented. Thus, the application and development of heterostructure Mg−Li alloys can receive positive feedback. It also makes Mg−Li alloys more widely used in aerospace, military industry, transportation, medical, and other fields.

(3) In the following work, more advanced analysis methods will be used to determine the slip (such as $\langle a \rangle$ basal slip and $\langle c+a \rangle$ pyramidal slip in α-Mg) and twining (such as $\{10\bar{1}1\}-\{10\bar{1}2\}$ double twins) mechanism during the deformation process of Mg−Li alloys, and reveal intrinsic relationship among the composition, microstructure, structure, and properties of Mg−Li alloys, to propose a more effective method (deformation, heat treatment or both) to significantly improve the mechanical properties of Mg−Li alloys.

CRediT authorship contribution statement

Zhan LIU: Investigation, Methodology, Writing − Origin-draft, Writing − Review & editing; **Jin-feng NIE:** Investigation, Conceptualization, Funding acquisition, Supervision, Writing – Review & editing; **Yong-hao ZHAO:** Supervision, Writing – Review & editing.

Declaration of competing interest

The authors declare that they have no known competing financial interests or personal relationships that could have appeared to influence the work reported in this paper.

Acknowledgments

The authors are grateful to the National Natural Science Foundation of China (Nos. 52071179, 5227010325), the Natural Science Foundation of Jiangsu Province, China (No. BK20221493) and the Fundamental Research Funds for the Central Universities, China (Nos. 30920021160, 30919011405).

References

[1] WU Guo-hua, WANG Cun-long, SUN Ming, DING Wen-jiang. Recent developments and applications on high-performance cast magnesium rare-earth alloys [J]. Journal of Magnesium and Alloys, 2021, 9(1): 1−20.

[2] DING Zhen-sen, FANG Hai-feng, LIU Bin, YAO Zhan-hui, LIU Jin-zhou. Research on the optimal scheme of 3E game for lightweight body-in-white under environmental protection policy [J]. Advances in Mechanical Engineering, 2021, 13(8): 1−16.

[3] PENG Xiang, LIU Wen-cai, WU Guo-hua. Alloying and application of Mg−Li alloys: A review [J]. The Chinese Journal of Nonferrous Metals, 2021, 31(11): 3024−3043. (in Chinese)

[4] MORDIKE B L, EBERT T. Magnesium: Properties−applications−potential [J]. Materials Science and Engineering A, 2001, 302(1): 37−45.

[5] ABDULLAEV R N, KHAIRULIN R A, KOZLOVSKII Y M, AGAZHANOV A S, STANKUS S V. Density of magnesium and magnesium-lithium alloys in solid and liquid states [J]. Transactions of Nonferrous Metals Society of China, 2019, 29(3): 507−514.

[6] BYRER T G, WHITE E L, FROST P D. Development of magnesium-lithium alloys for structural applications [R]. USA: George C. Marshall Space Flight Center of the National Aeronautics and Space Administration, 1964: 1−11.

[7] ELKIN F M, DAVYDOV V G. Russian ultralight constructional Mg−Li alloys. Their structure, properties,

manufacturing, applications [C]//Magnesium: Proceedings of the 6th International Conference Magnesium Alloys and Their Applications. Weinheim, Germany: Wiley-VCH Velag GmbH and Co. KGaA, 2003: 95−90.

[8] SINGH R K, MISHRA R S. Influence of minor additions of Zr on the mechanical behaviour of a Mg/1bLi/1bAl alloy [J]. Scripta Metallurgica et Materialia, 1990, 24(3): 451−456.

[9] GUO Xu-ying, WU Rui-zhi, ZHANG Jing-huai, LIU Bin, ZHANG Mi-lin. Influences of solid solution parameters on the microstrucuture and hardness of Mg−9Li−6Al and Mg−9Li−6Al−2Y [J]. Materials & Design, 2014, 53: 528−533.

[10] SHENG Dong-dong, SHI Ying-jie, WANG Xi-xi, XU Li, SUM Yu. The research status and trend of ultra-light Mg−Li alloy [J]. Light Alloy Fabrication Technology, 2021, 49(8): 8−12. (in Chinese)

[11] KULEKCI M K. Magnesium and its alloys applications in automotive industry [J]. The International Journal of Advanced Manufacturing Technology, 2008, 39(9): 851−865.

[12] SALDAU P, SCHAMRAY F. Equilibrium diagram of the magnesium-lithium system [J]. Zeitschrift Für Anorganische Und Allgemeine Chemie, 1935, 224(4): 388−398. (in German)

[13] HERBSTEIN F H, AVERBACH B L. The structure of lithium−magnesium solid solutions—I: Measurements on the Bragg reflections [J]. Acta Metallurgica, 1956, 4(4): 407−413.

[14] PENG Xiang, SUN Jia-wei, LIU Hong-jie, WU Guo-hua, LIU Wen-cai. Microstructure and corrosion behavior of as-homogenized and as-extruded Mg−*x*Li−3Al−2Zn−0.5Y alloys (*x*=4, 8, 12) [J]. Transactions of Nonferrous Metals Society of China, 2022, 32(1): 134−146.

[15] CHAKRAVORTY C R. Development of ultra light magnesium−lithium alloys [J]. Bulletin of Materials Science, 1994, 17(6): 733−745.

[16] YANG Yan, XIONG Xiao-ming, CHEN Jing, PENG Xiao-dong, CHEN Dao-lun, PAN Fu-sheng. Research advances in magnesium and magnesium alloys worldwide in 2020 [J]. Journal of Magnesium and Alloys, 2021, 9(3): 705−747.

[17] LI Xiao-qiang, CHENG Chun-long, LE Qi-chi, ZHOU Xiong, LIAO Qi-yu, CHEN Xing-rui, JIA Yong-hui, WANG Ping. Ex-situ EBSD analysis of yield asymmetry, texture and twinning development in Mg−5Li−3Al−2Zn alloy during tensile and compressive deformation [J]. Journal of Alloys and Compounds, 2019, 805: 947−956.

[18] LV Bin-jiang, PENG Jian, WANG Yong-jian, AN Xiao-qin, ZHONG Li-ping, TANG Ai-tao, PAN Fu-sheng. Dynamic recrystallization behavior and hot workability of Mg−2.0Zn−0.3Zr−0.9Y alloy by using hot compression test [J]. Materials & Design, 2014, 53: 357−365.

[19] LI Xiao-qiang, REN Liang, LE Qi-chi, JIN Pei-peng, CHENG Chun-long, WANG Tong, WANG Ping, ZHOU Xiong, CHEN Xing-rui, LI Dan-dan. The hot deformation behavior, microstructure evolution and texture types of as-cast Mg−Li alloy [J]. Journal of Alloys and Compounds, 2020, 831: 154868.

[20] WANG Jia-hao, WU Rui-zhi, FENG Jing, ZHANG Jing-huai, HOU Le-gan, ZHANG Mi-lin. Influence of rolling strain on electromagnetic shielding property and mechanical properties of dual-phase Mg−9Li alloy [J]. Materials Characterization, 2019, 157: 109924.

[21] KARAMI M, MAHMUDI R. Hot shear deformation constitutive analysis and processing map of extruded Mg−12Li−1Zn bcc alloy [J]. Materials & Design, 2014, 53: 534−539.

[22] DONG Han-wu, WANG Li-min, LIU Ke, WANG Li-dong, JIANG Bin, PAN Fu-sheng. Microstructure and deformation behaviors of two Mg−Li dual-phase alloys with an increasing tensile speed [J]. Materials & Design, 2016, 90: 157−164.

[23] PENG Xiang, LIU Wen-cai, WU Guo-hua. Effects of Li content on microstructure and mechanical properties of as-cast Mg−*x*Li−3Al−2Zn−0.5Y alloys [J]. Transactions of Nonferrous Metals Society of China, 2022, 32(3): 838−849.

[24] SUN Yue-hua, WANG Ri-chu, PENG Chao-qun, WANG Xiao-feng. Effect of Gd on microstructure, mechanical properties, and corrosion behavior of as-homogenized Mg−8Li−3Al−2Zn−0.2Zr alloy [J]. Transactions of Nonferrous Metals Society of China, 2022, 32(8): 2494−2509.

[25] CHEN Xiao-yang, ZHANG Yang, CONG Meng-qi, LU Ya-lin, LI Xiao-ping. Effect of Sn content on microstructure and tensile properties of as-cast and as-extruded Mg−8Li−3Al−(1,2,3)Sn alloys [J]. Transactions of Nonferrous Metals Society of China, 2020, 30(8): 2079−2089.

[26] KIM Y H, SON H T. Effects of Li addition on microstructure and mechanical properties of Mg−6Al−2Sn−0.4Mn alloys [J]. Transactions of Nonferrous Metals Society of China, 2016, 26(3): 697−703.

[27] WANG Yong-qing, ZHOU Zhi-yan, ZHOU Wen-zheng, XU Li-qin, GUO Jin, LAN Zhi-qiang. Effects of in-situ formed Mg_2Si phase on the hydrogen storage properties of MgLi solid solution alloys [J]. Materials & Design, 2016, 111: 248−252.

[28] WANG Jia-hao, SUN Dong-peng, WU Rui-zhi, DU Chun-lin, YANG Zhen-zhao, ZHANG Jing-huai, HOU Le-gan. A good balance between mechanical properties and electromagnetic shielding effectiveness in Mg−9Li−3Al−1Zn alloy [J]. Materials Characterization, 2022, 188: 111888.

[29] ESTRIN Y, NENE S S, KASHYAP B P, PRABHU N, AL-SAMMAN T. New hot rolled Mg−4Li−1Ca alloy: A potential candidate for automotive and biodegradable implant applications [J]. Materials Letters, 2016, 173: 252−256.

[30] DING Hong-bo, LIU Qiang, ZHOU Hai-tao, ZHOU Xiao, ATRENS A. Effect of thermal-mechanical processing on microstructure and mechanical properties of duplex-phase Mg−8Li−3Al−0.4Y alloy [J]. Transactions of Nonferrous Metals Society of China, 2017, 27(12): 2587−2597.

[31] CHIU Chui-Hung, WU Horng-Yu, WANG Jian-Yih, LEE Shyong. Microstructure and mechanical behavior of LZ91 Mg alloy processed by rolling and heat treatments [J]. Journal of Alloys and Compounds, 2008, 460(1/2): 246−252.

[32] QU Zhi-kun, WU Li-bin, WU Rui-zhi, ZHANG Jing-huai, ZHANG Mi-lin, LIU Bin. Microstructures and tensile properties of hot extruded Mg−5Li−3Al−2Zn−*x*RE (rare earths) alloys [J]. Materials & Design (1980—2015), 2014, 54: 792−795.

[33] LIU Teng, ZHANG Wei, WU Shi-ding, JIANG Chuan-bing, LI Shou-xin, XU Yong-bo. Mechanical properties of a two-phase alloy Mg−8%Li−1%Al processed by equal channel

angular pressing [J]. Materials Science and Engineering A, 2003, 360(1/2): 345−349.

[34] YANG Yue, CHEN Xiang, NIE Jin-feng, WEI Kang, MAO Qing-zhong, LU Feng-hua, ZHAO Yong-hao. Achieving ultra-strong magnesium−lithium alloys by low-strain rotary swaging [J]. Materials Research Letters, 2021, 9(6): 255−262.

[35] DUTKIEWICZ J, KALITA D, MAZIARZ W, FARYNA M. Superplastic deformation of Mg−9Li−2Al−0.5Sc alloy after grain refinement by KoBo extrusion and cyclic forging [J]. Archives of Civil and Mechanical Engineering, 2020, 20(4): 1−11.

[36] JOLLY M, KATGERMAN L. Modelling of defects in aluminium cast products [J]. Progress in Materials Science, 2022, 123: 100824.

[37] YUAN Guang-yu, YOU Guo-qiang, BAI Shi-lei, GUO Wei. Effects of heat treatment on the thermal properties of AZ91D magnesium alloys in different casting processes [J]. Journal of Alloys and Compounds, 2018, 766: 410−416.

[38] MA A B, NISHIDA Y, SAITO N, SHIGEMATSU I, LIM S W. Movement of alloying elements in Mg−8.5wt.%Li and AZ91 alloys during tensile tests for superplasticity [J]. Materials Science & Technology, 2003, 19(12): 1642−1647.

[39] CAO Han-xue, LONG Si-yuan, YOU Guo-qiang, LIAO Hui-min. Closing and repairing process of Mg alloy casting imperfections in plastic deformation [J]. The Chinese Journal of Nonferrous Metals, 2009, 19(7): 1176−1181. (in Chinese)

[40] GUO Fei, JIANG Lu-yao, MA Yan-long, LIU Lei, ZHANG Zhen, YANG Ming-bo, ZHANG Ding-fei, PAN Fu-sheng. Strengthening a dual-phase Mg−Li alloy by strain-induced phase transformation at room temperature [J]. Scripta Materialia, 2020, 179: 16−19.

[41] TIAN Jing, LU Hui-hu, ZHANG Wang-gang, NIE Hui-hui, SHI Quan-xin, DENG Jia-fei, LIANG Wei, WANG Li-fei. An effective rolling process of magnesium alloys for suppressing edge cracks: Width-limited rolling [J]. Journal of Magnesium and Alloys, 2022, 10(8): 2193−2207.

[42] KARHAUSEN K F, PAWELSKI H. Mechanics and friction in metal rolling [M]//MANG T. Encyclopedia of Lubricants and Lubrication. Berlin, Heidelberg: Springer, 2014: 1122−1136.

[43] LI Xin-yu, XIA Wei-jun, CHEN Ji-hua, YAN Hong-ge, LI Zhen-zhen, SU Bin, SONG Min. Dynamic recrystallization, texture and mechanical properties of high Mg content Al−Mg alloy deformed by high strain rate rolling [J]. Transactions of Nonferrous Metals Society of China, 2021, 31(10): 2885−2898.

[44] CAO Fu-rong, ZHOU Bi-jin, DING Xin, ZHANG Jian, XU Guang-ming. Mechanical properties and microstructural evolution in a superlight Mg−7.28Li−2.19Al−0.091Y alloy fabricated by rolling [J]. Journal of Alloys and Compounds, 2018, 745: 436−445.

[45] GUO Fei, LIU Lei, MA Yan-long, JIANG Lu-yao, ZHANG Yu-he, ZHANG Ding-fei, PAN Fu-sheng. Slip behavior and its effect on rolling texture development in a dual-phase Mg−Li alloy [J]. Journal of Alloys and Compounds, 2020, 813: 152117.

[46] LIU Wen-cai, FENG Shi, LI Zhong-quan, ZHAO Jiong, WU Guo-hua, WANG Xian-fei, XIAO Lv, DING Wen-jiang. Effect of rolling strain on microstructure and tensile properties of dual-phase Mg−8Li−3Al−2Zn−0.5Y alloy [J]. Journal of Materials Science & Technology, 2018, 34(12): 2256−2262.

[47] LI Yong-xiong, XIAO Chuan-jun, ZHANG A-peng. Effects of cold rolling deformation on microstructure and properties of Mg−9Li−1Zn alloy [J]. Hot Working Technology, 2020, 49(9): 78−80. (in Chinese)

[48] ZHONG Feng, WANG Yang, WU Rui-zhi, ZHANG Jing-huai, HOU Le-gan, ZHANG Mi-lin. Effect of rolling temperature on deformation behavior and mechanical properties of Mg−8Li−1Al−0.6Y−0.6Ce alloy [J]. Journal of Alloys and Compounds, 2020, 831: 154765.

[49] LI Xiao-yan, GUO Fei, MA Yan-long, JIANG Lu-yao, LAI Hong-liang, LIU Hai-ding, ZHANG Ding-fei, PEI Ri-sheng. Rolling texture development in a dual-phase Mg−Li alloy: The role of temperature [J]. Journal of Magnesium and Alloys, 2023, 11(8): 2980−2990.

[50] JIANG Wen-xiao, KUAI Zhi-ming, ZHU Lv-qi, ZHOU Hai-tao. Effect of asymmetrical rolling on microstructure and mechanical properties of Mg−8Li−3Al−0.4Ca alloy sheets [J]. Heat Treatment Technology and Equipment, 2019, 40(1): 33−38. (in Chinese)

[51] LIU Hong-yu, WANG Yang, LI Bing-cheng, MA Xiao-chun, WU Rui-zhi, HOU Le-gan, ZHANG Jing-huai, ZHANG Mi-lin. Effect of cryogenic rolling process on microstructure and mechanical properties of Mg−14Li−1Al alloy [J]. Materials Characterization, 2019, 157: 109903.

[52] MAO Qing-zhong, LIU Yan-fang, ZHAO Yong-hao. A review on mechanical properties and microstructure of ultrafine grained metals and alloys processed by rotary swaging [J]. Journal of Alloys and Compounds, 2022, 896: 163122.

[53] WAN Ying-chun, TANG Bei, GAO Yong-hao, TANG Ling-ling, SHA Gang, ZHANG Bo, LIANG Ning-ning, LIU Chu-ming, JIANG Shu-nong, CHEN Zhi-yong, GUO Xue-yi, ZHAO Yong-hao. Bulk nanocrystalline high-strength magnesium alloys prepared via rotary swaging [J]. Acta Materialia, 2020, 200: 274−286.

[54] CHEN Wen-huan, HE Wei-jun, JIANG Bin, LIU Qing, PAN Fu-sheng. Study on the compressive deformation behavior of a basal textured AZ31 magnesium alloy from the perspective of local strain [J]. Materials Science and Engineering A, 2022, 842: 143080.

[55] ESTRIN Y, MARTYNENKO N, LUKYANOVA E, SEREBRYANY V, GORSHENKOV M, MOROZOV M, YUSUPOV V, DOBATKIN S. Effect of rotary swaging on microstructure, texture, and mechanical properties of a Mg−Al−Zn alloy [J]. Advanced Engineering Materials, 2020, 22(1): 900506.

[56] GAN Wei-min, HUANG Yuan-ding, WANG R, ZHONG Zheng-ye, HORT N, KAINER K U, SCHELL N, BROKMEIER H G, SCHREYER A. Bulk and local textures of pure magnesium processed by rotary swaging [J]. Journal of Magnesium and Alloys, 2013, 1(4): 341−345.

[57] CHEN Xin, LIU Chu-ming, JIANG Shu-nong, CHEN Zhi-yong, WAN Ying-chun. Fabrication of nanocrystalline high-strength magnesium−lithium alloy by rotary swaging [J]. Advanced Engineering Materials, 2021, 24(1): 100666.

[58] YANG Guo-qing, PENG Xiao-dong, YANG Yan, LI Meng-luan, WEI Guo-bing, SHAO Hong-yan, WANG Bao. Microstructure and mechanical properties of as-cast and extruded Mg−8Li−3Al−0.7Si alloy [J]. Journal of Central

South University, 2018, 25(4): 764−771.

[59] HU Zhi, YIN Zheng, YIN Zhou, TANG Bin-bing, HUANG Xiao, YAN Hong, SONG Hong-gun, LUO Chao, CHEN Xiao-hui. Influence of Sm addition on microstructural and mechanical properties of as-extruded Mg−9Li−5Al alloy [J]. Journal of Alloys and Compounds, 2020, 842: 155836.

[60] HU Zhi, YIN Zheng, YIN Zhou, WANG Kun, LIU Qi-dong, SUN Peng-fei, YAN Hong, SONG Hong-gun, LUO Chao, GUAN Hong-yu, LUC C. Corrosion behavior characterization of as extruded Mg−8Li−3Al alloy with minor alloying elements (Gd, Sn and Cu) by scanning Kelvin probe force microscopy [J]. Corrosion Science, 2020, 176: 108923.

[61] KARAMI M, MAHMUDI R. Hot shear deformation constitutive analysis of an extruded Mg−6Li−1Zn alloy [J]. Materials Letters, 2012, 81: 235−238.

[62] KARAMI M, MAHMUDI R. Work hardening behavior of the extruded and equal-channel angularly pressed Mg−Li−Zn alloys under tensile and shear deformation modes [J]. Materials Science and Engineering A, 2014, 607: 512−520.

[63] KARAMI M, MAHMUDI R. Orientation-dependent microstructure and shear flow behavior of extruded Mg−Li−Zn alloys [J]. Materials Science and Engineering A, 2015, 636: 493−501.

[64] AYMAN E, JUNKO U, KATSUYOSHI K. Application of rapid solidification powder metallurgy to the fabrication of high-strength, high-ductility Mg−Al−Zn−Ca−La alloy through hot extrusion [J]. Acta Materialia, 2011, 59(1): 273−282.

[65] JIANG Bing-chun, WANG Shu-ping, LIU Fang-fang, TANG Lian-yao, LI Zhen-zhen. Effect of extrusion ratio on microstructure and mechanical properties of LZ92 duplex magnesium lithium alloy [J]. Nonferrous Metals Engineering, 2017, 7(1): 20−24. (in Chinese)

[66] JI Hao, WU Guo-hua, LIU Wen-cai, SUN Jiang-wei, DING Wen-jiang. Role of extrusion temperature on the microstructure evolution and tensile properties of an ultralight Mg−Li−Zn−Er alloy [J]. Journal of Alloys and Compounds, 2021, 876: 160181.

[67] TANG Yan, LE Qi-chi, MISRA R D K, SU Guan-qiao, CUI Jian-zhong. Influence of extruding temperature and heat treatment process on microstructure and mechanical properties of three structures containing Mg−Li alloy bars [J]. Materials Science and Engineering A, 2018, 712: 266−280.

[68] YANG Yan, XIONG Xiao-ming, SU Jun-fei, PENG Xiao-dong, WEN Hai-ming, WEI Guo-bing, PAN Fu-sheng, LAVERNIA E J. Influence of extrusion temperature on microstructure and mechanical behavior of duplex Mg−Li−Al−Sr alloy [J]. Journal of Alloys and Compounds, 2018, 750: 696−705.

[69] FENG Shi, LIU Wen-cai, ZHAO Jiong, WU Guo-hua, ZHANG Hao-hao, DING Wen-jiang. Effect of extrusion ratio on microstructure and mechanical properties of Mg−8Li−3Al−2Zn−0.5Y alloy with duplex structure [J]. Materials Science and Engineering A, 2017, 692: 9−16.

[70] LI Shuo-shuo, CHEN Liang, TANG Jian-wei, ZHAO Guo-qun, ZHANG Cun-sheng. Microstructure and mechanical properties of hot extruded Mg−8.89Li−0.96Zn alloy [J]. Results in Physics, 2019, 13: 102148.

[71] DONG Han-wu, PAN Fu-sheng, JIANG Bin, ZENG Ying. Evolution of microstructure and mechanical properties of a duplex Mg−Li alloy under extrusion with an increasing ratio [J]. Materials & Design, 2014, 57: 121−127.

[72] LEI Xue, WANG Ri-chu, PENG Chao-qun, FENG Yan, SUN Yue-hua. Effect of hot extrusion on the microstructure, mechanical properties, and corrosion behavior of Mg−11Li−3Al−2Zn−1.5Nd−0.2Zr Alloy [J]. Transactions of the Indian Institute of Metals, 2019, 72(10): 2893−2899.

[73] ZHANG Yang, ZHANG Jie, WU Guo-hua, LIU Wen-cai, ZHANG Liang, DING Wen-jiang. Microstructure and tensile properties of as-extruded Mg−Li−Zn−Gd alloys reinforced with icosahedral quasicrystal phase [J]. Materials & Design (1980—2015), 2015, 66: 162−168.

[74] ZHANG Jie, ZHANG Yang, WU Guo-hua, LIU Wen-cai, ZHANG Liang, DING Wen-jiang. Microstructure and mechanical properties of as-cast and extruded Mg−8Li−3Al−2Zn−0.5Nd alloy [J]. Materials Science and Engineering A, 2015, 621: 198−203.

[75] XU Tian-cai, PENG Xiao-dong, JIANG Jun-wei, XIE Wei-dong, CHEN Yuan-fang, WEI Guo-bing. Effect of Sr content on microstructure and mechanical properties of Mg−Li−Al−Mn alloy [J]. Transactions of Nonferrous Metals Society of China, 2014, 24(9): 2752−2760.

[76] TOTH L S, GU Cheng-fan. Ultrafine-grain metals by severe plastic deformation [J]. Materials Characterization, 2014, 92: 1−14.

[77] BASHA D A, SAHARA R, SOMEKAWA H, ROSALIE J M, SINGH A, TSUCHIYA K. Interfacial segregation induced by severe plastic deformation in a Mg−Zn−Y alloy [J]. Scripta Materialia, 2016, 124: 169−173.

[78] AZUSHIMA A, KOPP R, KORHONEN A, YANG D Y, MICARI F, LAHOTI G D, GROCHE P, YANAGIMOTO J, TSUJI N, ROSOCHOWSKI A, YANAGIDA A. Severe plastic deformation (SPD) processes for metals [J]. CIRP Annals, 2008, 57(2): 716−735.

[79] EDALATI K, MASUDA T, ARITA M, FURUI M, SAUVAGE X, HORITA Z, VALIEV R Z. Room-temperature superplasticity in an ultrafine-grained magnesium alloy [J]. Scientific Reports, 2017, 7(1): 2662.

[80] KARAMI M, MAHMUDI R. Shear punch superplasticity in equal-channel angularly pressed Mg−12Li−1Zn alloy [J]. Materials Science and Engineering A, 2013, 576: 156−159.

[81] KARAMI M, MAHMUDI R. The microstructural, textural, and mechanical properties of extruded and equal channel angularly pressed Mg−Li−Zn alloys [J]. Metallurgical and Materials Transactions A, 2013, 44(8): 3934−3946.

[82] FURUI M, KITAMURA H, ANADA H, LANGDON T G. Influence of preliminary extrusion conditions on the superplastic properties of a magnesium alloy processed by ECAP [J]. Acta Materialia, 2007, 55(3): 1083−1091.

[83] MINÁRIK P, KRÁL R, PEŠIČKA J, CHMELÍK F. Evolution of mechanical properties of LAE442 magnesium alloy processed by extrusion and ECAP [J]. Journal of Materials Research and Technology, 2015, 4(1): 75−78.

[84] ZHILYAEV A P, LANGDON T G. Using high-pressure torsion for metal processing: Fundamentals and applications [J]. Progress in Materials Science, 2008, 53(6): 893−979.

[85] MATSUNOSHITA H, EDALATI K, FURUI M, HORITA Z. Ultrafine-grained magnesium−lithium alloy processed by high-pressure torsion: Low-temperature superplasticity and

potential for hydroforming [J]. Materials Science and Engineering A, 2015, 640: 443−448.

[86] SRINIVASARAO B, ZHILYAEV A P, GUTIÉRREZ-URRUTIA I, PÉREZ-PRADO M T. Stabilization of metastable phases in Mg−Li alloys by high-pressure torsion [J]. Scripta Materialia, 2013, 68(8): 583−586.

[87] CHEN Yu-yao, NIE Jin-feng, WANG Fang, YANG Hua-bing, WU Chong-chong, LIU Xiang-fa, ZHAO Yong-hao. Revealing hetero-deformation induced (HDI) stress strengthening effect in laminated Al−$(TiB_2+TiC)_p$/6063 composites prepared by accumulative roll bonding [J]. Journal of Alloys and Compounds, 2020, 815: 152285.

[88] NIE Jin-feng, LIU Ming-xing, WANG Fang, ZHAO Yong-hao, LI Yu-sheng, CAO Yang, ZHU Yun-tian. Fabrication of Al/Mg/Al composites via accumulative roll bonding and their mechanical properties [J]. Materials, 2016, 9(11): 951.

[89] LV Zheng, MAO C, MA S, WANG Jing-feng, YANG J, YANG Zhi-min, LIANG Qiu-shi. Microstructure and properties analysis of accumulative-roll-bonding-processed Mg−Li/Ta composites for shielding of high-energy electron [J]. Radiation Physics and Chemistry, 2022, 193: 109940.

[90] SAITO Y, TSUJI N, UTSUNOMIYA H, SAKAI T, HONG R G. Ultra-fine grained bulk aluminum produced by accumulative roll-bonding (ARB) process [J]. Scripta Materialia, 1998, 39(9): 1221−1227.

[91] YU Hai-liang, TIEU A K, LU Cheng, GODBOLE A. An investigation of interface bonding of bimetallic foils by combined accumulative roll bonding and asymmetric rolling techniques [J]. Metallurgical and Materials Transactions A, 2014, 45(9): 4038−4045.

[92] WEI Zhen, ZHENG Hai-peng, WU Rui-zhi, ZHANG Jing-huai, WU Hua-jie, JIN Si-yuan, JIAO Yun-lei, HOU Le-gan. Interface behavior and tensile properties of Mg−14Li−3Al−2Gd sheets prepared by four-layer accumulative roll bonding [J]. Journal of Manufacturing Processes, 2021, 61: 254−260.

[93] TSUJI N, SAITO Y, LEE S H, MINAMINO Y. ARB (accumulative roll-bonding) and other new techniques to produce bulk ultrafine grained materials [J]. Advanced Engineering Materials, 2003, 5(5): 338−344.

[94] ZHONG Feng, WANG Tian-zi, WU Rui-zhi, HOU Le-gan, ZHANG Jing-huai, LI Xin-lin, ZHANG Mi-lin, DONG An-ping, SUN Bao-de. Microstructure, texture, and mechanical properties of alternate α/β Mg−Li composite sheets prepared by accumulative roll bonding [J]. Advanced Engineering Materials, 2017, 19(5): 1600817.

[95] ZHENG Hai-peng, WU Rui-zhi, HOU Le-gan, ZHANG Jing-huai, ZHANG Mi-lin. Mathematical analysis and its experimental comparisons for the accumulative roll bonding (ARB) process with different superimposed layers [J]. Journal of Magnesium and Alloys, 2021, 9(5): 1741−1752.

[96] RAHMATABADI D, PAHLAVANI M, GHOLAMI M D, MARZBANRAD J, HASHEMI R. Production of Al/Mg−Li composite by the accumulative roll bonding process [J]. Journal of Materials Research and Technology, 2020, 9(4): 7880−7886.

[97] WANG Yang, LIAO Yang, WU Rui-zhi, TURAKHODJAEV N, CHEN Hong-tao, ZHANG Jing-huai, ZHANG Mi-lin, MARDONAKULOV S. Microstructure and mechanical properties of ultra-lightweight Mg−Li−Al/Al−Li composite produced by accumulative roll bonding at ambient temperature [J]. Materials Science and Engineering A, 2020, 787: 139494.

[98] WANG Jia-hao, XU Lin, WU Rui-zhi, AN Di, WEI Zhen, WANG Jia-xiu, FENG Jing, ZHANG Jing-huai, HOU Le-gan, LIU Mei-duo. Simultaneous achievement of high electromagnetic shielding effectiveness (X-band) and strength in Mg−Li−Zn−Gd/MWCNTs composite [J]. Journal of Alloys and Compounds, 2021, 882: 160524.

[99] WANG Jia-hao, WU Rui-zhi, FENG Jing, ZHANG Jing-huai, HOU Le-gan, LIU Mei-duo. Recent advances of electromagnetic interference shielding Mg matrix materials and their processings: A review [J]. Transactions of Nonferrous Metals Society of China, 2022, 32(5): 1385−1404.

[100] GUO Jie-wen, WANG Jun-li, ZHANG Tong-ying, ZHANG Su-peng. Microstructure and properties of LZ91 magnesium alloy processed by asynchronous accumulative roll bonding [J]. Materials Research Express, 2020, 7(12): 126513.

[101] SAUFAN A, YU I S, WANG J Y. Enhancement of mechanical properties for Mg−9Li−1Zn alloy by accumulative roll bonding [J]. Materials Research Express, 2020, 7(4): 046511.

[102] WANG Tian-zi, ZHENG Hai-peng, WU Rui-zhi, YANG Jin-liang, MA Xu-dong, ZHANG Mi-lin. Preparation of fine-grained and high-strength Mg−8Li−3Al−1Zn alloy by accumulative roll bonding [J]. Advanced Engineering Materials, 2016, 18(2): 304−311.

[103] WU Hua-jie, WANG Tian-zi, WU Rui-zhi, HOU Le-gan, ZHANG Jing-huai, LI Xin-lin, ZHANG Mi-lin. Microstructure and mechanical properties of Mg−5Li−1Al sheets processed by cross accumulative roll bonding [J]. Journal of Manufacturing Processes, 2019, 46: 139−146.

[104] HOU Le-gan, WANG Tian-zi, WU Rui-zhi, ZHANG Jing-huai, ZHANG Mi-lin, DONG An-ping, SUN Bao-de, BETSOFEN S, KRIT B. Microstructure and mechanical properties of Mg−5Li−1Al sheets prepared by accumulative roll bonding [J]. Journal of Materials Science & Technology, 2018, 34(2): 317−323.

[105] KHANI MOGHANAKI S, KAZEMINEZHAD M. Effects of non-isothermal annealing on microstructure and mechanical properties of severely deformed 2024 aluminum alloy [J]. Transactions of Nonferrous Metals Society of China, 2017, 27(1): 1−9.

[106] YANG Xu-yue, SUN Zheng-yan, XING Jie, MIURA H, SAKAI T. Grain size and texture changes of magnesium alloy AZ31 during multi-directional forging [J]. Transactions of Nonferrous Metals Society of China, 2008, 18(Suppl.): 200−204.

[107] DONG Bei-bei, CHE Xin, ZHANG Zhi-min, YU Jian-min, MENG Mu. Microstructure evolution and microhardness of Mg−13Gd−4Y−2Zn−0.5Zr alloy via pre-solution and multi-directional forging (MDF) process [J]. Journal of Alloys and Compounds, 2021, 853: 157066.

[108] CAO Fu-rong, XUE Guo-qiang, XU Guang-ming. Superplasticity of a dual-phase-dominated Mg−Li−Al−Zn−Sr alloy processed by multidirectional forging and rolling [J]. Materials Science and Engineering A, 2017, 704: 360−374.

[109] CAO Fu-rong, ZHANG Jian, DING Xin, XUE Guo-qiang, LIU Si-yuan, SUN Chao-feng, SU Rui-kang, TENG

Xiao-ming. Mechanical properties and microstructural evolution in a superlight Mg−6.4Li−3.6Zn−0.37Al−0.36Y alloy processed by multidirectional forging and rolling [J]. Materials Science and Engineering A, 2019, 760: 377−393.
[110] MINETA T, HASEGAWA K, SATO H. High strength and plastic deformability of Mg−Li−Al alloy with dual BCC phase produced by a combination of heat treatment and multi-directional forging in channel die [J]. Materials Science and Engineering A, 2020, 773: 138867.
[111] CAO Fu-rong, SUN Chao-feng, SHANG Hui-hui, XIANG Chao, LIU Ren-jie. Microstructure evolution and mechanical properties in an ultralight Mg−2.76Li−3Al−2.6Zn−0.39Y alloy [J]. Materials Science and Engineering A, 2021, 822: 141680.
[112] MA E, ZHU T. Towards strength−ductility synergy through the design of heterogeneous nanostructures in metals [J]. Materials Today, 2017, 20(6): 323−331.
[113] ZHU Yun-tian, WU Xiao-lei. Perspective on hetero-deformation induced (HDI) hardening and back stress [J]. Materials Research Letters, 2019, 7(10): 393−398.
[114] MEHRABI A, MAHMUDI R, MIURA H. Superplasticity in a multi-directionally forged Mg−Li−Zn alloy [J]. Materials Science and Engineering A, 2019, 765: 138274.
[115] MISHRA R S, MAHONEY M W, MCFADDEN S X, MARA N A, MUKHERJEE A K. High strain rate superplasticity in a friction stir processed 7075 Al alloy [J]. Scripta Materialia, 1999, 42(2): 163−168.
[116] MISHRA R S, MA Z Y. Friction stir welding and processing [J]. Materials Science and Engineering R: Reports, 2005, 50(1/2): 1−78.
[117] KADIAN A K, BISWAS P. Effect of tool pin profile on the material flow characteristics of AA6061 [J]. Journal of Manufacturing Processes, 2017, 26: 382−392.
[118] VICTOR CHRISTY J, ISMAIL MOURAD A H, SHERIF M M, SHIVAMURTHY B. Review of recent trends in friction stir welding process of aluminum alloys and aluminum metal matrix composites [J]. Transactions of Nonferrous Metals Society of China, 2021, 31(11): 3281−3309.
[119] RUANO O A, ALVAREZ-LEAL M, OROZCO-CABALLERO A, CARREÑO F. Superplasticity of a friction stir processed overaged WE54 magnesium alloy [J]. Journal of Magnesium and Alloys, 2022, 10(11): 3156−3166.
[120] MA Zong-yi, MISHRA R S, MAHONEY M W. Superplasticity in cast A356 induced via friction stir processing [J]. Scripta Materialia, 2004, 50(7): 931−935.
[121] MA Zong-yi, MISHRA R S, MAHONEY M W, GRIMES R. High strain rate superplasticity in friction stir processed Al−Mg−Zr alloy [J]. Materials Science and Engineering A, 2003, 351(1/2): 148−153.
[122] ZHOU Meng-ran, MORISADA Y, FUJII H, WANG J Y. Microstructure and mechanical properties of friction stir welded duplex Mg−Li alloy LZ91 [J]. Materials Science and Engineering A, 2020, 773: 138730.
[123] MORISADA Y, FUJII H, KANDA K, KUBOTA K, ISAKA M. Evaluation of friction stir welding tool using wettability [J]. Welding International, 2018, 32(7): 469−474.
[124] LIU Gang, MA Zhen-duo, WEI Guo-bing, XU Tian-cai, ZHANG Xi, YANG Yan, XIE Wei-dong, PENG Xiao-dong. Microstructure, tensile properties and corrosion behavior of friction stir processed Mg−9Li−1Zn alloy [J]. Journal of Materials Processing Technology, 2019, 267: 393−402.
[125] LI Yi, GUAN Yan-jin, LIU Ya, ZHAI Ji-qiang, HU Kai, LIN Jun. Effect of processing parameters on the microstructure and tensile properties of a dual-phase Mg−Li alloy during friction stir processing [J]. Journal of Materials Research and Technology, 2022, 17: 2714−2724.
[126] ZHOU Meng-ran, ZENG Zhuo-ran, CHENG Chun, MORISADA Y, SHI Qing-yu, WANG J Y, FUJII H. Effect of the processing route on the microstructure and mechanical behavior of superlight Mg−9Li−1Zn alloy via friction stir processing [J]. Journal of Magnesium and Alloys, 2022, 10(11): 3064−3081.

变形处理对 Mg−Li 合金显微组织演变和力学性能的影响

刘 站，聂金凤，赵永好

南京理工大学 材料科学与工程学院 纳米异构材料中心，南京 210094

摘 要：镁锂合金具有较高的比强度和比刚度、优秀的电磁屏蔽效应和阻尼性能等优点，是目前最轻的金属结构材料，在自动化、航空、交通运输、医疗等领域有广泛的应用前景。但是，和其他金属结构材料相比，镁锂合金的强度仍然偏低，需要对镁锂合金进行合金化或者变形处理来提高力学性能。总结了各类变形处理镁锂合金的研究现状，讨论了常规变形加工和剧烈塑性变形加工对镁锂合金显微组织和力学性能的影响，并总结了变形加工过程中形变量和温度对显微组织和力学性能的影响，以及镁锂合金的几种晶粒细化机制，阐述了镁锂合金在工业应用中遇到的问题。晶粒细化和加工硬化目前仍然是提高镁锂合金性能的主要手段。强调了几种变形和结构设计(异质材料)，这将有助于镁锂合金的创新工作，从而得到高强度镁锂合金。

关键词：镁锂合金；显微组织；力学性能；塑性变形；细晶强化；剧烈塑性变形

(Edited by Bing YANG)